

LYMPH NODE AND PERI-LYMPH NODE STROMA: PHENOTYPE  
AND INTERACTION WITH T-CELLS

Nicholas J. Stoffel

Submitted to the faculty of the University Graduate School  
in partial fulfillment of the requirements  
for the degree  
Master of Science  
in the Department of Microbiology and Immunology,  
Indiana University

December 2013

Accepted by the Graduate Faculty, Indiana University, in partial fulfillment of the requirements for the degree of Master of Science.

Master's Thesis Committee

---

Christopher E. Touloukian, M.D., Chair

---

Hal E. Broxmeyer, Ph.D.

---

Edward F. Srouer, Ph.D.

---

David A. Ingram Jr., M.D.

## ACKNOWLEDGEMENTS

I wish to express my sincere gratitude to everyone who has helped and guided me through my graduate program. Dr. Christopher Touloukian has been an experienced and trusted mentor, advising me in experimental design, data analysis, and professional growth. He has been an excellent teacher of immunology. I also extend my heartfelt appreciation to my former and current lab members for their assistance with experiments and protocols – Emily Sturm, Roy Chen, Ariel Gallanosa, and especially Garrett Kinnebrew. From the flow cytometry core I would like to thank Kimberly Stoner and Susan Rice for their patience, time, and assistance. I would also like to thank Momoko Yoshimoto for her guidance in differentiating T cell progenitors using OP9-DL1 cells. Dr. Robert Bacallao was of extremely helpful in his knowledge and guidance in staining histology slides. LeAnne Baldrige of the Pathology department was also very instrumental in helping with histology slides. I want to acknowledge my committee members – Drs. Hal Broxmeyer, Edward Srouf, and David Ingram for their time and valuable input. Committee meetings were fruitful and provided me with ideas and experimental plans. Cindy Booth has been extremely helpful in assisting me with many problems. I would like to also thank the IBMG program and the staff who have always assisted with care. It has been a privilege to be a student at Indiana University School of Medicine. I sincerely thank everyone who has helped me with this achievement.

Nicholas J. Stoffel

LYMPH NODE AND PERI-LYMPH NODE STROMA: PHENOTYPE AND INTERACTION WITH T-CELLS

The non-hematopoietic, stationary stromal cells located inside and surrounding skin-draining lymph nodes play a key role in regulating immune responses. We studied distinct populations of lymph node stromal cells from both human subjects and animal models in order to describe their phenotype and function. In the mouse model, we studied two distinct populations: an endothelial cell population expressing Ly51 and MHC-II, and an epithelial cell population expressing the epithelial adhesion molecule EpCAM. Analysis of intra-nodal and extra-nodal lymph node (CD45-) stromal cells through flow cytometry and qPCR provides a general phenotypic profile of the distinct populations. My research focused on the EpCAM+ epithelial cell population located in the fat pad surrounding the skin draining lymph nodes. The EpCAM+ population has been characterized by surface marker phenotype, anatomic location, and gene expression profile. This population demonstrates the ability to inhibit the activation and proliferation of both CD4 and CD8 T cells. This population may play a role in suppressing overactive inflammation and auto-reactive T cells that escaped thymic deletion. The other major arm of my project consisted of identifying a novel endothelial cell population in human lymph nodes. Freshly resected lymph nodes were processed into single cell suspensions and selected for non-hematopoietic CD45- stromal cells. The unique endothelial population expressing CD34 HLA-DR was then characterized and analyzed for anatomic position, surface marker expression, and gene profiles. Overall, these studies emphasize the importance of stationary lymph node stromal cells to our functioning immune systems, and may have clinical relevance to autoimmune diseases, inflammation, and bone marrow transplantation.

Christopher E. Touloukian, M.D., Chair

## TABLE OF CONTENTS

LIST OF FIGURES.....	vi
LIST OF ABBREVIATIONS .....	ix
INTRODUCTION.....	1
EXPERIMENTAL PLAN.....	9
CHAPTER 1. MOUSE LYMPH NODE STROMA.....	12
Introduction .....	12
Materials and Methods.....	17
Results.....	25
CHAPTER 2. HUMAN LYMPH NODE STROMA.....	45
Introduction .....	45
Materials and Methods.....	46
Results.....	54
DISCUSSION AND FUTURE DIRECTIONS.....	73
Chapter 1. Lymph Node Stroma of the Mouse.....	73
Chapter 2. Human Lymph Node Stroma.....	79
REFERENCES.....	82
CURRICULUM VITAE	

LIST OF FIGURES

INTRODUCTION

Figure 1. Lymph node stroma vs T cell co-culture setup and analysis..... 11

CHAPTER 1. MOUSE LYMPH NODE STROMA

Figure 2. Methylene blue injection of mouse foot pad ..... 13

Figure 3. Flow cytometry of two distinct mouse lymph node stromal cell populations: EpCAM+ and Ly51+ cells ..... 14

Figure 4. Fat versus follicle analysis in mouse skin draining lymph nodes ..... 16

Figure 5. Antibodies used for mouse analysis ..... 20

Figure 6. Introductory descriptive analysis of Ly51+ and EpCAM+ cells ..... 26

Figure 7. Immunofluorescent microscopy of freshly isolated EpCAM+ cells..... 27

Figure 8. Histological microscopy of the fat pad surrounding the inguinal lymph node follicle in BL/6J mice ..... 29

Figure 9. Flow cytometric analysis of CD45-/EpCAM+ cell surface markers (adhesion and costimulation) ..... 30

Figure 10. Flow cytometric analysis of CD45-/EpCAM+ cell markers [stem-like, MSC-like (mesenchymal stem cell), and miscellaneous] ..... 32

Figure 11. Day 4 culture of EpCAM+ cells in RPMI 10% FBS ..... 34

Figure 12. Day 12 growth of EpCAM+ cells on irradiated 3T3's increases growth potential ..... 35

Figure 13. 8 Day growth of EpCAM+ cells plated on confluent, irradiated LA7 rat mammary cells ..... 36

Figure 14. Ly51+ lymph node stromal cells can uptake Ova and cross-present to naïve OT-I T cells ..... 38

Figure 15. EpCAM+ cells demonstrate the ability to inhibit the proliferation of bead-activated CD4 and CD8 T cells in a dose-dependent manner .....	39
Figure 16. EpCAM+ cells can keep bead-activated T cells in their naïve state. ....	40
Figure 17. EpCAM+ lymph node stromal cells inhibit the production of IL-2 in a dose dependent manner .....	41
Figure 18. Inhibition of T cells by EpCAM+ lymph node stroma: contact mediated or secretion-dependent .....	43
Figure 19. EpCAM+ cells up-regulate potential T cell inhibitory genes IDO and iNOS in response to secreted factors released by bead-activated T cells.....	44
<b>CHAPTER 2. HUMAN LYMPH NODE STROMA</b>	
Figure 20. Antibodies used for human analysis .....	48
Figure 21. Human lymph node digest and flow cytometric profile .....	55
Figure 22. Analysis of HLA-DR+ CD34+ surface profile (part 1) .....	56
Figure 23. Analysis of HLA-DR+ CD34+ flow cytometric profile (part 2) .....	58
Figure 24. qRT-PCR (Panel 1 – Positive Flow Controls and Growth Factors) – Relative expression (%Gapdh) of genes using in 3 populations: Adipose Derived Stem Cells (ADSCs), CD34+HLA-DR-, and CD34+HLA-DR+ .....	60
Figure 25. qRT-PCR (Panel 2 – Surface Receptors) .....	61
Figure 26. qRT-PCR (Panel 3 – Cytokines and Chemokines) .....	63
Figure 27. qRT-PCR (Panel 4 – Antigen Processing and Promiscuous Self-Antigens) .....	65
Figure 28. qRT-PCR (Panel 5 – T Cell Development and IL3R Downstream Signaling) .....	67
Figure 29. Patient 2 lymph node and surrounding tissue histology .....	70
Figure 30. Growth attempts of human CD34+ HLA-DR+ lymph node cells .....	71
Figure 31. Growth attempts of human CD34+ HLA-DR+ cells (Flow Cytometry) .....	72

DISCUSSION AND FUTURE DIRECTIONS

Figure 32. Proposed model of the inhibitory action of EpCAM+ cells on activated T

cells ..... 78



## LIST OF ABBREVIATIONS

1-MT	1-methyl-tryptophan
3T3	Swiss Mouse Embryonic Fibroblast Cell Line
Ab	Antibody
ABS	Applied Biosystems
ADSCs	Adipose-derived Stem Cells
AG	Aminoguanidine Hydrochloride
AIRE	Auto-immune Regulator gene
$\alpha$	anti-
APC	Antigen Presenting Cell
ARG1	Arginase
ASCs	Adipose-derived Stem Cells
BEC	Blood Endothelial Cell
bFGF	Basic Fibroblast Growth Factor
BG	Betagalactosidase
Bgal	Betagalactosidase
BL/6	C57BL/6J mice
BM	Bone Marrow
c-KIT	Stem Cell Factor Receptor (SCFR) (CD117)
CD	Cluster of Differentiation
CD11c	Marker for Dendritic Cells
CD3	Pan T cell surface marker
cDNA	Complementary Deoxyribonucleic Acid
CFSE	Carboxyfluorescein succinimidyl ester
CLP	Common Lymphoid Progenitor

CTLA-4	Cytotoxic T-Lymphocyte Antigen 4
CXCL12	Chemokine (C-X-C motif) Ligand 12 (SDF-1 )
CXCR4	Chemokine Receptor for SDF-1
DAPI	4',6-Diamidino-2-Phenylindole, Dihydrochloride
DC	Dendritic Cell
DISC	death-inducing signaling complex
DLL1	Delta-like Protein 1
DLL4	Delta-like Protein 4
DN	Double Negative
DP	Double Positive
e	$\times 10^n$ power
EGF	Epidermal Growth Factor
EGFR	Epidermal Growth Factor Receptor
EpCAM	Epithelial Cell Adhesion Molecule
ETPs	Early T cell Progenitors
FACS	Fluorescence-Activated Cell Sorting
FADD	Fas-associated death domain protein
Fas	TNF-receptor
FasL	Fas-ligand
FBS	Fetal Bovine Serum
FDC	Follicular Dendritic Cell
FGF	Fibroblast Growth Factor
FGFR	Fibroblast Growth Factor Receptor
Flt-3	FMS-like tyrosine kinase 3
FLT3L	FMS-like Tyrosine Kinase 3 Ligand

FRC	Fibroblastic Reticular Cell
FSC	Forward Scatter
GAPDH	Glyceraldehyde 3-phosphate Dehydrogenase
GC	Guanine Cytosine
GCSF	Granulocyte Colony-Stimulating Factor
gp	Glycoprotein
gp38	Membrane Glycoprotein (Podoplanin)
h	Human
HEV	High Endothelial Venule
HLA	Human Leukocyte Antigen
HSCs	Hematopoietic Stem Cells
IACUC	Institutional Animal Care and Use Committee
IC	Intracellular
ICOS	Inducible T-cell Costimulator (CD278)
ICOS-L	Inducible T-cell Costimulator Ligand (CD275)
IDO	Indoleamine 2,3-dioxygenase
IDO1	Indoleamine 2,3-dioxygenase
IFN- $\gamma$	Interferon gamma
IFNGR	Interferon Gamma Receptor
IGF1	Insulin-like Growth Factor 1
IGF1R	Insulin-like Growth Factor 1 Receptor
IHC	Immunohistochemistry
IL	Interleukin
iNOS	Inducible Nitric Oxide Synthase (NOS2)
IRB	Institutional Review Board

IU	Indiana University
IUSM	Indiana University School of Medicine
K	x1000
KITL	Stem Cell Factor (SCF) binds c-Kit receptor
KLF4	Kruppel-like factor 4 Demonstrates Stem-like Capacity
LA7	Sprague-Dawley Adult Female Rat Mammary Tumor Cell Line
LEC	Lymphetic Endothelial Cell
LIF	Leukemia Inhibitory Factor
LIFR	Leukemia Inhibitory Factor Receptor
Lin-	Lineage Negative (Lacks lineage commitment markers)
LN	Lymph Nodes
LSK	Lin <sup>-</sup> Sca-1 <sup>High</sup> c-Kit <sup>High</sup>
LTB	Lymphotoxin Beta
LtBR	Lymphotoxin Beta Receptor
Ly51	Glutamyl Aminopeptidase Surface Antigen also known as BP-1
m	Mouse/murine
MACS	Magnetic Assisted Cell Sorting (Miltenyi)
MFI	Mean Fluorescence Intensity
MHC	Major Histocompatibility Complex
mRNA	Messenger RNA
MSC	Mesenchymal Stem Cell
MSCs	Mesenchymal Stem Cells
mTECs	Medullary Thymic Epithelial Cells
MYC	Transcription Factor
N	Naive T cells

NANOG	Transcription Factor
NIH	National Institute of Health
NO	Nitric Oxide
NOS2	Nitric Oxide Synthase (inducible) gene
4-Oct	Octamer-binding Transcription Factor 4 (POU5F1)
OT-I	T cells isolated from C57BL/6-Tg(TcraTcrb)1100Mjb/J mice with TCRs specific to ovalbumin peptide 257-264 in the context of MHC-I
OT-II	T cells isolated from B6.Cg-Tg(TcraTcrb)425Cbn/J with TCRs specific to ovalbumin peptide 323-339 in the context of MHC-II
Ova	Ovalbumin
P	Passage
PCK	Pan-Cytokeratin
PCR	Polymerase Chain Reaction
PD-1	Programmed Cell Death 1
PDL1	Programmed Cell Death 1 Ligand 1, CD274
PDL2	Programmed Cell Death 1 Ligand 2, CD273
pep	Peptide
qPCR	Quantitative Real-Time Polymerase Chain Reaction
RBC	Red Blood Cell
RNA	Ribonucleic Acid
RPM	Revolutions Per Minute
RPMI	Roswell Park Memorial Institute Media
Sca-1	Marker for Bone Marrow Progenitor Cells
SDF-1	Stromal Derived Factor-1
SMA	Smooth Muscle Actin

SOX2	Sex Determining Region Y - Box 2 Transcription Factor
SP	Single Positive
SSC	Side Scatter
STAT1	Signal Transducer and Activator of Transcription 1
TCR	T Cell Receptor
TGFB	Transforming Growth Factor Beta
TNF	Tumor Necrosis Factor
TNFR	Tumor Necrosis Factor Receptor
Tyrp1	Surface Protein Present on Melanocytes
VEGF	Vascular Endothelial Growth Factor

## INTRODUCTION

Stromal cells inside and surrounding the lymph node play a major role in T cell stimulation and regulation. Lymph nodes are the major site of antigen presentation by antigen presenting cells (APCs) to T cells [1]. The lymph node stromal cells have been previously described in detail [2, 3], but the stromal cells surrounding the lymph node have not been clearly characterized. Our lab has analyzed both human and mouse lymph nodes and the surrounding tissue to identify and phenotype cell populations of interest, characterized these populations, and to investigate the functional properties of these cell populations.

To understand how we identified our populations of interest one must look at our original focus of research. Initially, we wanted to compare the thymic stromal cells to the intra-follicular and extra-follicular lymph node stroma. Thymic stromal cells are responsible for the education and maturation of developing T cells. The thymic stromal cells are capable of presenting a variety of promiscuously expressed tissue-specific self-antigen and presenting it to self-reactive T cells for deletional tolerance [4]. We speculated that self-reactive T cells which escape the thymus without deletional tolerance need a mechanism of control in the periphery. We hypothesized that the lymph node stromal cells could serve a similar role as the thymic stromal cells in regulating or deleting self-reactive T cells in the peripheral blood.

### **T Cell Development and Self-Antigen Tolerance**

During T cell development, hematopoietic stem cells (HSCs) originating in the bone marrow (BM) differentiate into T-lineage progenitors such as the early T-lineage progenitor (ETPs) or the common lymphoid progenitor (CLP) [5]. ETPs express a surface phenotype similar to the BM multipotent progenitors, Lin<sup>-</sup>Sca-1<sup>High</sup>c-Kit<sup>High</sup> (LSK), but express low levels of IL-7R $\alpha$  [6] and the

majority lack FMS-like tyrosine kinase 3 (Flt3) expression [7, 8]. These T cell progenitors then migrate to the thymus for proliferation and development.

### **Thymic Cortex Stroma's Role in T Cell Positive Selection**

In the thymic cortex, early T cells lack CD4, CD8, and T cell Receptor (TCR) and are termed double negative (DN) T cells [9]. DN T cells are named according to their progression in development. DN1 T cells have the surface markers CD44+CD25-; DN2, CD44+CD25+; DN3, CD44-CD25+; DN4, CD44-CD25- [10]. DN4 T cells become double positive (DP) T cells expressing genetically rearranged heterodimeric TCR- $\alpha\beta$  and both CD4 and CD8 [11]. The notch delta homologs DLL1 and DLL4 (Delta-like ligand), present on thymic stromal cells, play a major role in T cell maturation and development[12]. They contribute to the environment and signaling processes necessary for immature T cells to undergo maturation. Zúñiga-Pflücker et al. in 2002 demonstrated that the bone marrow stromal cell line OP9, ectopically expressing DLL1, could inhibit B cell differentiation and stimulate T cell differentiation from hematopoietic progenitor cells[13].

T cells undergo positive selection in the thymic cortex: T cells that have functional TCRs and are capable of interacting with MHC (major histocompatibility complex)/HLA (Human leukocyte antigen) are positively selected for survival and become single positive (SP) T cells, either CD4 or CD8; while those T cells with nonfunctional TCRs or TCRs that do not recognize or bind only weakly to MHC/HLA complexes undergo apoptosis[14]. The cortical thymic epithelial cells (cTECs), which characteristically express surface markers CD45-EpCAM+ Ly51+ MHCII+[15], are responsible for presentation of MHC/HLA complexes to the developing T cell and signaling with



tyrosine kinase Lck molecules for positive selection and survival of the MHC/HLA reactive SP T cell[16].

### **Thymic Medula Stroma's Role in T Cell Negative Selection and Education**

Following positive selection in the thymic cortex, SP T cells migrate to the thymic medulla, via CCR7 dependent signaling, to undergo further education and tolerance to self-antigen[17]. An important stromal cell contained in the thymic medulla is the medullary thymic epithelial cell (mTEC). The surface profile of mTECs is CD45- EpCAM+ Ly51- MHCII+ [15]. The autoimmune regulator gene AIRE, expressed in mTECs, drives the expression of a multitude of peripheral-tissue restricted antigens [18, 19]. These peripheral-tissue restricted antigens are presented in the cleft of the mTECs' MHC/HLA complexes to maturing T cells. When a T cell is auto-reactive against the self-antigen a signaling cascade involving Bcl-2 is activated, resulting in apoptosis of the auto-reactive T cell [20]. This process of negative selection is essential for limiting the number of auto-reactive T cells that escape the thymus into the periphery. Another method of eliminating self-reactive T cells enrolls thymic dendritic cells (DCs) which are also capable of signaling apoptosis of self-reactive T cells based on presentation of self-antigen to specific TCRs [21].

### **Escape of Auto-reactive T Cells from the Thymus**

Despite the positive and negative selection measures of the thymus, in healthy individuals self-reactive T cells do escape the thymus and migrate to the periphery[22]. The exact mechanism of self-reactive T cell escape is unknown. It is possible that not all self-antigens are presented to T cells via DCs or mTECs, or that the self-antigens presented are not sufficient in deleting self-reactive T cells[23]. The self-reactive T cells that escape thymus negative selection may not

have TCRs with strong enough affinity to self-antigen, this being supported by the study showing that auto-reactive T cells in the periphery have a tendency to bear low affinity TCRs to self-antigen[24]. Since auto-reactive T cells escape the thymus and travel to the periphery, there must be a mechanism for suppressing the immune response against self-antigen.

### **Peripheral Tolerance Mechanisms**

Peripheral tolerance can take many shapes and forms including circulating T regulatory cells, anergy through lack of costimulation, and expression of promiscuous self-antigen by lymph node stromal cells. The key to these mechanisms is inhibiting auto-reactive T cells by making them functionally inactive or outright killing or inducing apoptosis.

T cells require a two-step stimulation in order to be fully active and functional. The first signal necessary is the engagement of the TCR with an APC's MHC complex in conjunction with the TCR's specific antigen, and the second signal is a nonspecific interaction between co-stimulatory molecules such as the T cell's CD28 and the APC's CD80 or CD86. Without this co-stimulation, the T cells are anergized, made functionally inactive, and are unable to proliferate leading to a lack of IL-2 production and a suppression of the immune response[25]. With normal T cell co-stimulation IL-2 is released from the T cell and proliferation occurs.

Another method of inhibiting T cells in the periphery is induction of apoptosis. One signaling pathway that leads to apoptosis is the Fas-FasL pathway. Select populations of APCs have the Fas-ligand (FasL) protein present on their surface[26] which can then bind Fas present on T cells inducing T cell suicide. When inactive Fas on T cells ligates with FasL on APCs, Fas reorganizes forming the death-inducing signaling complex (DISC) which contains the Fas-associated death

domain protein (FADD) and caspases 8 and 10, which are responsible for the cascade leading to apoptosis of T cells[27].

T cells can also be inhibited by ligand binding to the immune-inhibitory receptor PD-1 found on the surface of select T cell populations. PD-1 will down-regulate T cell responses and when knocked-out can lead to auto-immune type diseases such as lupus[28]. PD-1 can bind molecules in the B7 family (CD80/CD86/PD-L1) present on APCs leading to down-regulation of the immune response[29].

Regulatory T cells (Tregs) also play a major role in peripheral tolerance of self-antigen. Naturally occurring Tregs mature in the thymus and express the following surface profile: CD4+ CD25+ Foxp3+ (transcription factor forkhead box p3)[30]. When released into the periphery, Tregs are responsible for the negative regulation and suppression of immune reactions. They also play a major role in prevention of autoimmune diseases[31].

Thymic stromal cells are not the only cell type to express the transcription factor AIRE, which is responsible for driving the expression of many promiscuous self-antigens. The auto-reactive T cells that escape thymic negative selection could travel to the periphery where stromal cells located in the lymph node can present self-antigen and mediate deletion of auto-reactive T cells [32]. It has also been shown that self-reactive T cells located in the periphery and presented with self-antigen can be induced to down-regulate TCRs [33]. This secondary network of self-antigen presentation and negative selection may play a major role in peripheral tolerance.

Lymphotoxin  $\beta$  Receptor (LtBR) is present in lymph node stroma and plays a key role in the development of lymph nodes with their interaction with lymphotoxin  $\beta$  and  $\alpha$  present on lymphocytes[34]. LtBR signaling can induce stromal cells to produce IL-8, an inducer of inflammation and a chemotactic factor for neutrophils [35]. We hypothesized that the LtBR present on lymph node stromal cells may play a role in suppressing T cells in the periphery through an unknown mechanism.

Two additional suppressive mechanisms that may be responsible for suppression of T cell activation and/or proliferation are indoleamine 2, 3-dioxygenase 1 (IDO1) and inducible nitric oxide synthase (iNOS). When T cell activation occurs in the presence of co-stimulation IFN- $\lambda$  production can be induced [36]. When T cells are activated IFN- $\lambda$  is released and can induce nearby cells to upregulate IDO1 [37] and iNOS [38]. IDO1 catalyzes the conversion of tryptophan, an essential amino acid necessary for T cell proliferation, to kynurenine. This depletion of tryptophan inhibits T cell proliferation [39] while the kynurenine can induce apoptosis [40]. Human bone marrow stromal cells and dendritic cells have both been shown to inhibit T cells through this mechanism [39, 41]. iNOS is an inducible nitric oxide synthase encoded by the NOS2 gene. iNOS produces nitric oxide (NO) as a byproduct when converting L-arginine to citrulline. iNOS upregulation and enhancement can occur by signaling from TNF- $\alpha$  [42] and IFN- $\gamma$  [43]. NO is toxic due to its ability to combine with superoxides to form peroxynitrites; a free radical capable of damaging DNA, lipids, and proteins [44]. NO is also capable of suppressing T cell proliferation [45].

## **Lymph Node Stroma and Their Current Classification**

Lymph nodes are secondary lymphoid organs found throughout the body and are important to the immune system. The lymph nodes are essentially scaffolds and filters for collecting lymph fluid containing antigens, APCs, T cells, and B cells from the circulating lymphatic system.

Circulating APCs such as dendritic cells or B cells will phagocytize invading bacteria, process and present antigen, and migrate to the lymph node to present antigen to T helper lymphocytes causing activation. Activated T helper cells will bind antigen presented by B lymphocytes in the context of MHCII, activating the B lymphocyte and causing the B cell to mature into an antibody producing plasma cell. Virus infected cells or damaged cells will also migrate to the lymph node and present antigen in the context of MHCI to T cytotoxic lymphocytes, causing the T cells to be activated. Activated T cytotoxic lymphocytes will then proliferate, migrate, and target cells (with the specific antigen their TCRs recognize) for destruction [46].

The structure of the lymph node can be divided into two main regions: the medulla and the cortex. Lymph fluid enters the lymph node via afferent lymphatic vessels and then drains through cellular filters to collect cells and antigens before exiting the lymph node via the efferent lymphatic vessels located at the hilum near the medulla [1]. B cells are initially activated in the T cell rich zones in the paracortex of the lymph node, and migrate to the outer cortex to form germinal centers. Here, B cells undergo maturation into plasma cells to produce antibodies to the specific antigen in question[46].

The four main groups of stromal cells located within the lymph node: fibroblastic reticular cells (FRCs), lymphatic endothelial cells (LECs), blood endothelial cells (BECs), and the follicular dendritic cells (FDCs) have been classified by other investigators. These CD45- cells can be

differentiated by the presence or absence of two surface markers: gp38 and CD31. FRCs, gp38+CD31-; LECs, gp38+CD31+; BECs, gp38-CD31+; FDCs, gp38-CD31- [47]. These four classifications of stromal cells will be used as guidelines, but our lymph node preparation includes the surrounding fat, which have characteristically larger number of stroma and different characteristics.

The fibroblastic reticular cells (located in the lymph node cortex) are responsible for secreting chemotactic factors such as IL-7, CCL19, and CCL21 to assist T cell migration through the lymph node [48]. FRCs also express LtBR, an essential molecule in lymph node development and maturation[49].

LECs form the afferent and efferent lymphatic vessels that allow the flow of lymph fluid into and out of the lymph node. They have the surface markers VEGFR-3 (the receptor for vascular endothelial growth factors VEGF-C and VEGF-D), LYVE-1 (a receptor for hyaluronan), and express Prox-1 (a homeobox transcription factor essential for remodeling vascular endothelial cells into LECs [50])[51].

BECs constitute the vascular system inside the lymph node as well as specialized high endothelial venules (HEVs) responsible for trafficking naïve T cells into the lymph node for adhesion [47, 52].

FDCs are different than normal DCs: they are not hematopoietically derived, they lack CD45, and they organize germinal centers inside the lymph node. FDCs also directly sustain the growth and differentiation of B cells located in the germinal centers [53].

## EXPERIMENTAL PLAN

Isolation of distinct lymph node stromal populations in both mouse and human tissues helped us to understand the role lymph node stromal cells play in regulating the immune system. In the murine model, we have isolated two distinct populations, a T cell activating Ly51+ MHC-II+ cell population (further referred to as Ly51+ cells) and a population of EpCAM+ cells capable of inhibiting T cell proliferation and activation. We believe these cells form a tight-knit regulatory system for controlling how T cells are activated and for the suppression of an overactive immune response. This dual control over T cell stimulation and proliferation is necessary to defend against hyper-inflammation and possibly auto-reactive T cells leading to auto-immune diseases.

We described, phenotypically and functionally, the role that lymph node stromal cells play. Our goals were fourfold: 1) Refine the protocol for isolating lymph node stromal cells. 2) Give a clear phenotypic profile of human and mouse lymph node stromal cells along with a gene expression profile. 3) Determine if the lymph node stromal cells were capable of up-taking foreign antigen, presenting this antigen to T cells and activating said T cells. 4) Determine if the epithelial (EpCAM+) cell population of interest plays a role in inhibiting T cell proliferation and activation; and if so, what is the mechanism of this inhibition?

Reproducible isolation of lymph node stromal cells has been described in detail previously [54], but we believe that our preparation (see Materials and Methods) releases more stromal cells than other protocols – benefiting yield and proportions of distinct populations. By using the novel classifications, EpCAM+ or Ly51+, of peri-lymph and lymph node stromal cell populations, the role of the differing populations can be better understood. The isolation of human lymph

node stroma and its characterization is poorly described in literature. We successfully phenotypically describe the populations found in the human lymph node based on the surface markers CD34 and HLA-DR.

With the Ly51+ MHC-II+ population found in the mouse, one must analyze the possible role this cell has in uptake and presentation of antigen to CD4 T cells. The MHC-II positivity denotes that this cell may be capable of up-taking exogenous antigen and stimulating CD4 T cells. Upon further investigation, we discovered that this cell is also capable of cross-presenting antigen in the context of MHC-I to CD8 T cells.

T cell activation and inhibition was determined using a co-culture with either Ly51+ or EpCAM+ cells to elicit the effect of these stromal cells on T cells (Figure 1). Activation, proliferation, and inhibition were measured with flow cytometry of surface marker known for activation (CD62L, CD44, CD25), and by measuring the proliferation using carboxyfluorescein succinimidyl ester (CFSE), a marker that is inherited to daughter cells after cell division. Proliferative and inhibitory effects were also measured by ELISAs detecting cytokine release into the supernatant of co-cultures. These experiments are designed to better elucidate the role of distinct lymph node stromal populations in regulating T cells.



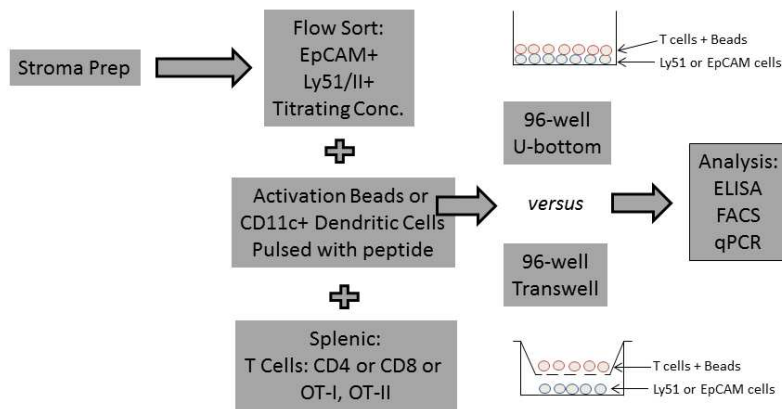


**Fig 1. Lymph node stroma vs T cell co-culture setup and analysis.** The above diagram demonstrates the method of co-culturing sorted stromal cells with T cells to demonstrate activation, proliferation, cytokine release, gene up-regulation, and inhibition. Sorted cells were placed in 96 well plates (U-bottom or transwell) at varying concentrations. CFSE-labeled T cells (CD4, CD8, OT-I, or OT-II) were placed into the same wells with the lymph node stromal cells. T cells were activated with either CD3/CD28/CD137 Dynabeads® (Life Technologies, Carlsbad, CA) or CD11c+ dendritic cells pulsed with the appropriate peptide to stimulate a recall response from ovalbumin sensitized OT-I or OT-II T cells. Flow analysis of T cell activation markers was conducted prior to co-culture. The co-culture was incubated at 37°C for 3-7 days depending on the experiment in question. Supernatants were harvested for ELISA analysis and cells were analyzed for mRNA up-regulation with qRT-PCR or T cell activation and proliferation by Flow cytometry.

## CHAPTER 1. MOUSE LYMPH NODE STROMA

### **Introduction**

Two unique populations of lymph node stromal cells were identified in the tissue inside and surrounding the skin-draining lymph node follicles of the mouse. The skin-draining lymph nodes effectively pool APCs, T cells, and antigen into the same site to mount an effective immune response (Figure 2). Inguinal, axillary, and brachial skin draining lymph nodes along with their surrounding fat pads were removed from each mouse for analysis. Mechanical separation using the GentleMACS C tube along with the GentleMACS Dissociator (Miltenyi Biotec, Bergisch Gladbach, Germany) was essential for separating the tissue sufficiently enough for the digest to separate all stromal cells. Using the knowledge of surface markers present in the thymic epithelial cells, we used similar markers to identify and isolate two unique CD45- non-hematopoietic stromal cell populations within the lymph node and surrounding tissue (Figure 3). The viable CD45- population, which only represents approximately 20% of the cells in and around the lymph node, characterizes the lymph node and peri-lymph node stromal cells. When further gating on Ly51+ and EpCAM+ cell populations, three distinct populations of interest arise: the Ly51+ population (also found to be MHCII+, EpCAM+ population, and the Ly51-EpCAM- population. We focused our research on the Ly51+MHCII+ population and the EpCAM+ population. The Ly51+ population is roughly 70% of the CD45 negative stromal cells found in our tissue, while the EpCAM+ population is less frequent at approximately 15% of the total CD45- stromal cells. These are the populations of interest that will be the focus of the mouse lymph node experiments and analysis. While not containing the same populations as the thymus stroma, the lymph node stroma cells share some of the surface markers present in the invaluable eTEC and mTEC populations.

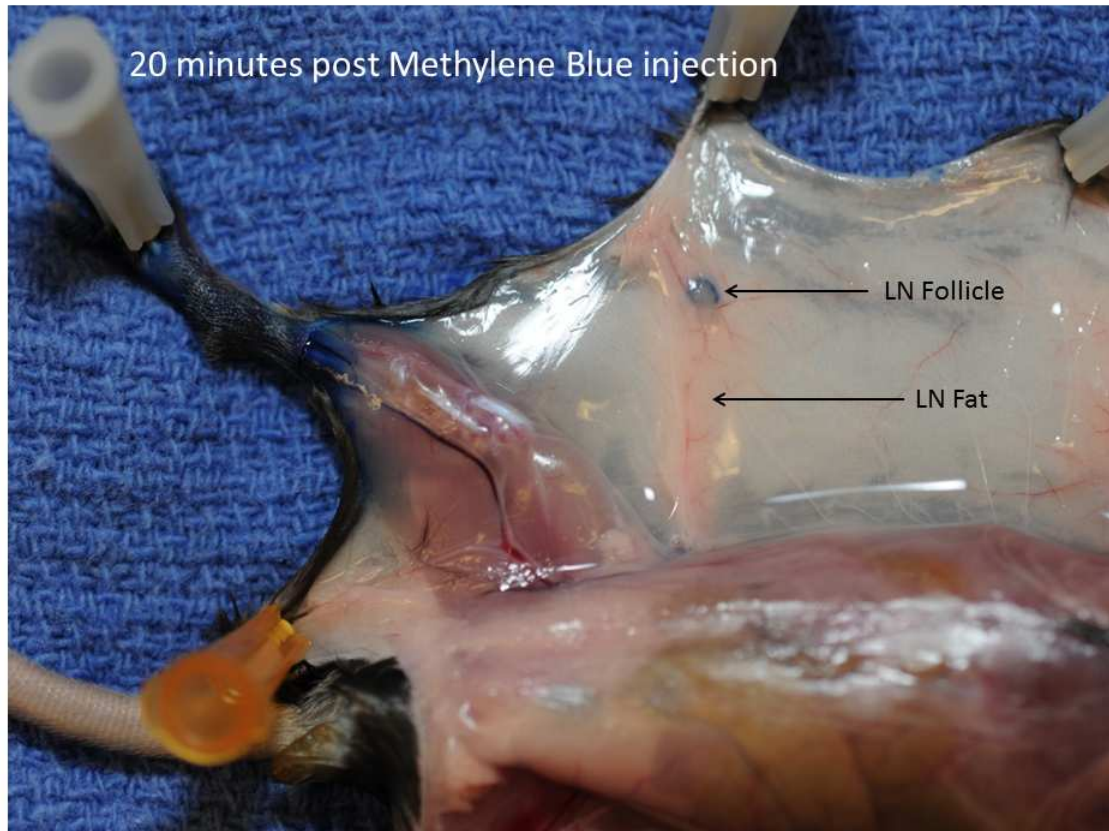


**Fig 2. Methylene blue injection of mouse foot pad.** Skin draining lymph nodes demonstrate the flow of lymph fluid from peripheral sites to specific lymph nodes. Shown above is the methylene blue tracking to the lymph node follicle in 20 minutes. Our studies included excising both the lymph node follicle and the surrounding fat. Shown above is the inguinal lymph node; the brachial and axillary lymph nodes were also excised along with their surrounding fat pads in all studies.

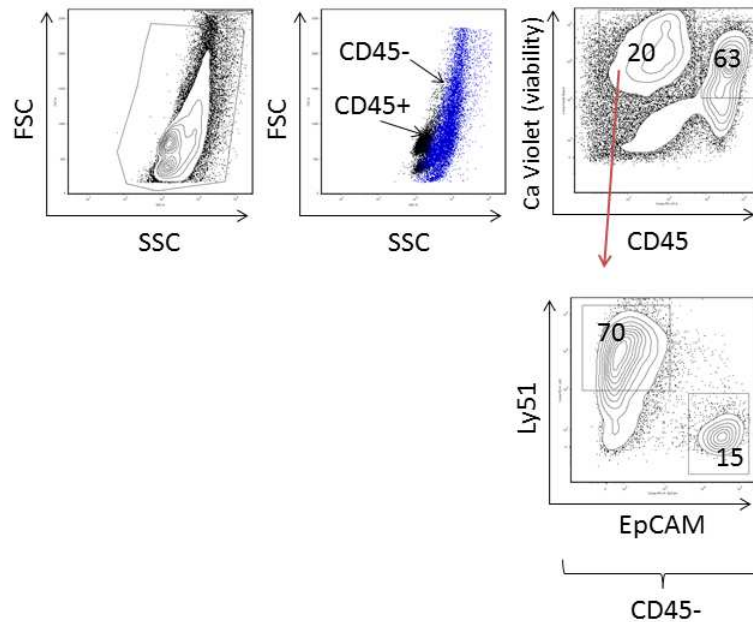


**Fig 3. Flow cytometry of two distinct mouse lymph node stromal cell populations: EpCAM+ and Ly51+ cells.** Following lymph node and peripheral lymph node fat excision, tissue was digested with collagenase D (Roche, Basel Switzerland) for 1 hour followed by RBC lysis and flow cytometry staining. 20% of the tissue is living CD45- cells (non-hematopoietic origin.) Calcein Violet (Ca Violet) is a viability stain which stains positive in living cells, demonstrating their intracellular esterase activity. Gating on the living CD45- cell population, there are 3 main populations of cells based on Ly51 and EpCAM staining: Ly51- EpCAM-, Ly51+ EpCAM-, and Ly51- EpCAM+. Our studies focused on the characteristics of the prevalent single positive Ly51+ populations and the less frequent single positive EpCAM+ populations.

In order to differentiate between the lymph node follicle and the surrounding fat, experiments were performed excising the lymph node follicle from the surrounding fat and processing the two tissues separately. Analysis of the lymph node follicle CD45- population (Figure 4) demonstrates that stromal cells are very sparse within the actual lymph node populations, at approximately .5% of the total number of cells. This small number of cells represents the stromal component of the lymph node. The surrounding fat pad around the follicle showed a large percentage of stromal cells at approximately 46% of the total number of cells. We hypothesized that this large number of stromal cells immediately surrounding the follicle must play a major role in the immune system and specifically in T cell activation and inhibition. Further analysis of the follicle and fat determined that the majority of the EpCAM+ cells reside extra-nodally, while the Ly51+ cells exist in both the lymph node follicle and extra-nodally. Further experiments combined lymph node follicle and fat to analyze the complex stroma as a whole. When sorting or isolation of EpCAM+ or Ly51+ cells occurred, the cells can be considered to be taken from the respective area with the higher concentration of this cell type. This was done because the percentage of EpCAM+ stromal cells in the lymph node was too low to have any representative effect on co-cultures or analysis and to elucidate the role of the stroma, as a whole, in effecting immune response.

EpCAM+ cells were the focus of my mouse stromal cell studies, while most research into the function of Ly51+ cells was being conducted by others in the laboratory.

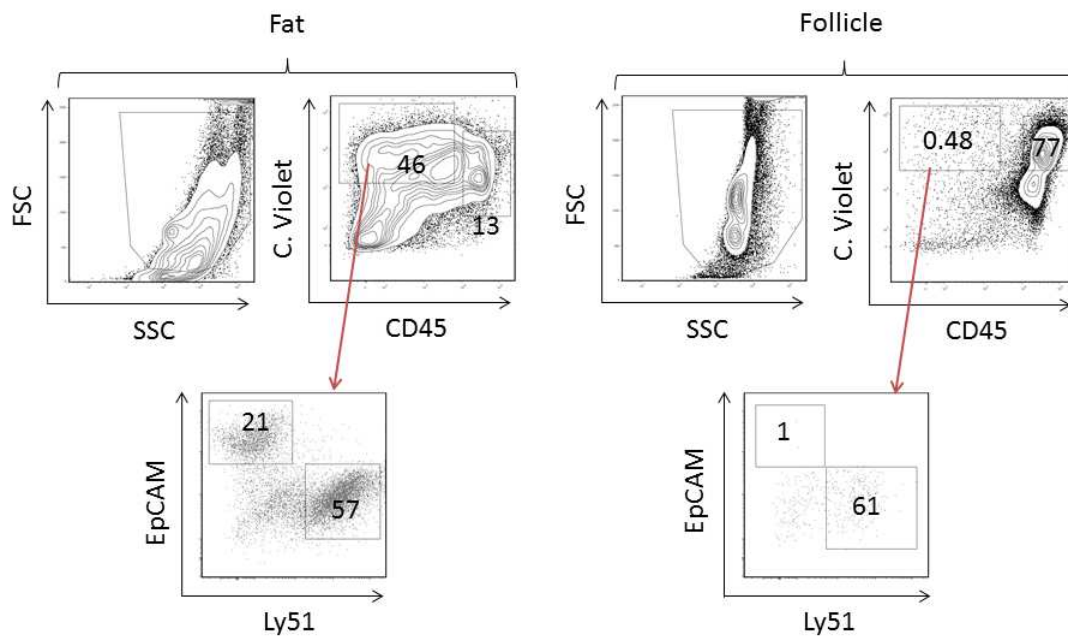


**Fig 4. Fat versus follicle analysis in mouse skin draining lymph nodes.** Lymph node stromal cells of nonhematopoietic origin (CD45-) are much more prevalent in the fat surrounding the actual lymph node follicle. 46% of the cells in the fat are CD45- while only 0.48 of cells in the lymph node are CD45-. This demonstrates that the lymph node stromal cells are mostly in the fat surrounding the follicle and that for experimental purposes and consistency, fat and follicle were excised and processed together to identify all stromal cell populations present.

## **Materials and Methods:**

### **Mice**

C57Bl/6, OT-I, and OT-II mice were purchased from Jackson Laboratory (Bar Harbor, ME) and housed in the Indiana University School of Medicine (IUSM) Animal Facility. All mouse experiments were approved by the Institutional Animal Care and Use Committee (IACUC).

### **Preparation of Lymph Node**

Axial, brachial, and inguinal skin draining lymph nodes were excised along with the surrounding fat pads unless otherwise indicated. Tissue was kept on ice unless otherwise indicated. Tissues from three mice were placed into one GentleMACS C tube (Miltenyi Biotec Inc., Auburn, CA) containing 3 mL of cold Hyclone RPMI (Thermo Scientific, Waltham, MA) supplemented with 10% Hyclone FBS, 100 I.U./mL Penicillin, 100 ug/mL Streptomycin, 1mM Sodium Pyruvate, 1x MEM Nonessential Amino Acids ((Mediatech, Manassas, VA), 2mM L-Glutamine, 20mM HEPES (Lonza, Walkersville, MD), and 1x 2-Mercaptoethanol (Gibco, Grand Island, NY) and dissociated using the GentleMACS Dissociator (Miltenyi Biotec Inc.) on default setting "spleen 02" (14 seconds). Any tissue remaining in the blades of the GentleMACS C tube was removed using forceps and placed into the remaining dissociated tissue. 10 ug Collagenase D (Roche, Basel, Switzerland) was dissolved in 2mL of supplemented RPMI and added to the 3 mL of RPMI containing the dissociated tissue for a final w/v of 0.2%. Lymph node tissue was incubated at 37°C (5% CO<sub>2</sub>) for 30 minutes, and then dissociated for 60 seconds with the GentleMACS Dissociator default setting "Spleen 01", again incubated for 30 minutes at 37°C, and finally dissociated again for 60 seconds using the "Spleen 01" setting. 45 mL of supplemented RPMI added to digested lymph node and transferred to a 50 mL conical tube and centrifuged at 400

RPM for 10 minutes. Supernatant was disposed and pellet was resuspended in 2 mL of 1x RBC Lysis Buffer (eBioscience) for 60 seconds and inactivated with 30 mL cold FACS buffer (2% FBS in Thermo Scientific PBS.) Suspension then filtered through a 40 um cell strainer (Thermo Scientific) and strainer rinsed with an additional 20 mL of FACS buffer. Cell suspension centrifuged at 350 RPM for 5 minutes and resuspended in FACS buffer for flow cytometry analysis or supplemented RPMI for growth studies or selected for CD45- cell populations using CD45 MicroBeads (Miltenyi Biotec, Bergisch Gladbach, Germany.) CD45 microbeads were added to the disaggregated cell populations, incubated at 4°C for 30 minutes, followed by 2 washes with MACS buffer and then a run through an LS column attached to a magnet and magnetic stand (Miltenyi Biotec.) Run through was collected and selected for Ly51+ or EpCAM+ cell populations using Ly51-biotin and EpCAM-biotin antibodies respectively, followed by a FACS buffer wash and staining with anti-biotin microbeads (Miltenyi Biotec, Bergisch Gladbach, Germany.) Cells were then positively selected LS columns from Miltenyi Biotec.

### **Flow Cytometry Analysis**

Antibodies were purchased from eBioscience (San Diego, CA) unless otherwise noted. Events were collected with the LSRII flow cytometer (BD Biosciences) at IUSM's Flow Cytometry Core. Antibodies were diluted at 1:100 of the tube volume with a minimum of 1uL of antibody and 100 uL of FACS buffer for every 1e6 cells. Antibodies were incubated at 4°C for 30 minutes and subsequently washed two times with FACS buffer and centrifuged for 5 minutes at 350RPM. Analysis was performed using FlowJo (Tree Star Inc., Ashland, OR.) Isotype controls and compensation controls used for every analysis. CellTrace™ Calcein Violet, AM (Invitrogen, Carlsbad, California), diluted 1:1000 used for cell viability. Intracellular staining was conducted using eBioscience intracellular staining protocol A with IC Fixation Buffer and Permeabilization



Buffer. CellTrace Carboxyfluorescein succinimidyl ester (CFSE) Proliferation Kit (Molecular Probes, Eugene, Oregon) was used for proliferation quantification. Cell sorting was conducted using the BD FACSAria (BD Biosciences) located at IUSM's Flow Cytometry Core. List of antibodies used (Figure 5).

<b>Epitope</b>	<b>Species</b>	<b>Isotype</b>	<b>Fluorophore</b>	<b>Clone</b>
Ly51	Mouse	IgG2a	PE	6C3
Ly51	Rat	IgG2a	FITC	6C3
Ly51	Rat	IgG2a	AF-647	6C3
EpCAM	Rat	IgG2a	APC	test2
EpCAM	Rat	IgG2a	FITC	G8.8
EpCAM	Rat	IgG2a	PE-Cy7	G8.8
EpCAM	Rat	IgG2a	Biotin	G8.8
Ly51	Rat	IgG1	Biotin	FG35.4
CD45	Rat	IgG2b	PE-Cy7	30-F11
PCK	Mouse	IgG1	AF-488	AE1/AE3
$\alpha$ -SMA	Mouse	IgG2a	FITC	1A4
CD31	Rat	IgG2a	PE	390
CD31	Rat	IgG2a	eF450	390
CD31	Rat	IgG2a	APC	390
CD31	Rat	IgG2a	AF-488	390
gp38	Hamster	IgG	PE	8.1.1
gp38	Hamster	IgG	AF-488	8.1.1
CD69	Hamster	IgG1	FITC	H1.2F3
CD69	Hamster	IgG1	APC	H1.2F3
CD4	Rat	IgG2a	PE	H129.19
CD4	Rat	IgG2b	APC	I3/2.3
CD4	Rat	IgG2b	PE-Cy7	GK1.5
CD4	Rat	IgG2b	FITC	GK1.5
CD8	Rat	IgG2a	FITC	53-6.7
CD8	Rat	IgG2a	PE	53-6.7
CD8	Rat	IgG2a	PacBlue	53-6.7
CD44	Rat	IgG2b	PE	IM7
CD44	Rat	IgG2b	APC	IM7
CD62L	Rat	IgG2a	APC	MEL-14
CD62L	Rat	IgG2a	FITC	MEL-14
CD62L	Rat	IgG2a	eF450	MEL-14
CD25	Rat	IgG1	AF-488	PC61.5
CD25	Rat	IgM	FITC	7D4

CD25	Rat	IgM	PE	7D4
CD25	Rat	IgG1	PE-Cy7	PC61
CD273 (PDL2)	Rat	IgG2a	None	122
CD274(PDL1)	Rat	IgG2b	APC	10F.9G2
LtBR (CD18)	Rat	IgG1	Biotin	eBioC38
LYVE-1	Rat	IgG1	eF660	ALY7
CD40	Rat	IgG2a	APC	1C10
CD54 (ICAM-1)	Hamster	IgG1	APC	3.00E+02
CD80 (B7-1)	Hamster	IgG	APC	16-10A1
CD86 (B7-2)	Rat	IgG2a	AF-647	GL-1
CD106 (VCAM-1)	Rat	IgG2a	AF-647	429
CD275 (ICOS-L)	Rat	IgG2a	None	HK5.3
CD38	Rat	IgG2a	AF-700	90
CD140a	Rat	IgG2a	APC	APA5
CD157	Mouse	IgG2b	APC	BP-3
CXCR4	Rat	IgG2b	APC	2B11
Sca-1	Rat	IgG2a	APC	D7
c-Kit	Rat	IgG2b	APC-eF780	2B8
CD9	Rat	IgG2a	FITC	KMC8
CD29	Hamster	IgG	APC	HMb1-1
MHC-I	Mouse	IgG2a	APC	AF6-88.5.5.3
MHC-II	Rat	IgG2b	FITC	M5/114.15.2
MHC-II	Rat	IgG2b	APC	M5/114.15.2
CD11c	Hamster	IgG1	PE	HL3
CD3	Rat	IgG2b	None	17A2

**Fig 5. Antibodies used for mouse analysis.**

#### **qRT-PCR Analysis**

Quantitative real time PCR was performed using lymph nodes and surrounding tissues digested and prepared as described. Cells were sorted for CD45- Calcein Violet+/EpCAM+ and CD45- Calcein Violet+/Ly51+MHCII+. 200,000 cells were used for preparation of each RNA sample. RNA was prepared using RNeasy Plus Mini Kit to the manufacturers specifications (Qiagen, Venlo, Limburg.) cDNA was reverse transcribed from isolated RNA using the High Capacity cDNA

Reverse Transcription Kit (Invitrogen, Carlsbad, CA) according to the manufacturer's protocol. SYBR Green PCR Master Mix (Applied Biosystems, Foster City, CA) or TaqMan Real Time PCR Master Mixes (Life Technologies, Carlsbad, CA) were used for the qPCR reaction according to the manufacturer's protocol. Samples were run on the STEPOne PLUS Real Time qPCR System (Applied Biosystems). All primers were designed using PrimerBlast software (NIH) using the following requirements: PCR product size, 70-150; primer melting temperatures minimum, 58.0; optimum, 60.0; maximum, 60.0; maximum temperature melting difference, 2; exon should span an exon-exon junction; Guanine Cytosine (GC) content, 30-36; maximum polynucleotides, 3; maximum self-complementation, 5, 3 in a row; concentration of monovalent cations, 60; both primers need the same melting temperature[55]. The following 25 nmol oligonucleotide DNA primers were ordered from Integrated DNA Technologies: miL-10, 5'- ACT TTA AGG GTT ACT TGG GTT GC -3' and 5'- CAG CTT CTC ACC CAG GGA AT -3'; mTGFB1, 5'- ACG TCA CTG GAG TTG TAC GG -3' and 5'- GGG CTG ATC CCG TTG ATT TC -3' ; mPDL1, 5'- TCA CTT GCT ACG GGC GTT TA -3' and 5'- CCC AGT ACA CCA CTA ACG CA -3' ; mPDL2, 5'- GCT GCA TGT TCT GGA ATG CT -3' and 5'- TTG GGT TCC ATC CGA CTC AG -3'; mIDO1, 5'- AGT GCA GTA GAG CGT CAA GA -3' and 5'- GGT CCA CAA AGT CAC GCA TC -3'; mCTLA-4, 5'- CCC AGT CTT CTC TGA AGC CAT -3' and 5'- TTT GGT CAT TTG TCT GCC GC -3'; miNOS, 5'- AGG CCA CAT CGG ATT TCA CT -3' and 5'- TAG GCT TGT CTC TGG GTC CT -3'; mARG1, 5'- GTA CAT TGG CTT GCG AGA CG -3' and 5'- TTT CTT CCT TCC CAG CAG GT -3'; mARG2, 5'- GCA AAT TCC TTG CGT CCT GA -3' and 5'- TCC ACT CCT AGC TTC TTC TGT C -3'; miFNg, 5'- ACA CTG CAT CTT GGC TTT GC -3' and 5'- GCT TTC AAT GAC TGT GCC GT -3'; mDLL1, 5'-ACT GCA CTG ACC CAA TCT GT-3' and 5'-GGA GAC AAC CTG GGT ATC GG-3'; mDLL4, 5'-AGT GAG AAG CCA GAG TGT CG-3' and 5'-TGC CTT ATA CCT CTG TGG CAA-3'; mFLT3L, 5'-TCA ATC TTC AGG ACG AGA AGC A-3' and FGF5'- TTT GCA TCT TAG ACC CTG CCA-3'; mKITL, 5'-GGT CCC GAG AAA GAT TCC AGA-3' and 5'-CCA TTG TAG GCC CGA GTC TT-3'; miL7, 5'-AGG AAC TGA TAG TAA

TTG CCC GA-3' and 5'-AGC AGC TTC CTT TGT ATC ATC AC-3'; mIFNGR1, 5'TGC CTG TAC CGA CGA ATG TT-3' and 5'-TCC AGG AAC CCG AAT ACA CC-3'; mTNFRSF1A, 5'-CAG TGA GGT AGT CCC AAC CC-3' and 5'-ATC GCA AGG TCT GCA TTG TC-3'; mTNFRSF1B, 5'-GTT CTT CCT GTA CCA CTG ACC A-3' and 5'-CAA GCA CAC ACT CGG TTC TG-3'; mEGFR, 5'-TAC CTA TGG ATG TGC TGG GC-3' and 5'-ACT GCC ATT GAA CGT ACC CA-3'; mIGF1R, 5'-GCG AGC TTC CTG TGA AAG TG-3' and 5'-GAT GAG ATC CCG GTA GTC CG-3'; mFGF1R, 5'-ATG ACG ACG ACG ATG ACT CC-3' and 5'-GGG AGC TAC AGG GTT TGG TT-3'; mLIFR, 5'-ACT GTG TTC ATT TGG AGG CAT-3' and 5'-TCA GTC AGC CCT CTC ACA AG- 3'; mKIT, 5'- ACT GGT GGT TCA GAG TTC CA-3' and 5'-GGC CTG GAT TTG CTC TTT GT-3'; mMYC, 5'-CCT GTA CCT CGT CCG ATT CC-3' and 5'-TGC TCT TCT TCA GAG TCG CT-3'; mNANOG, 5'-AAA GGA TGA AGT GCA AGC GG-3' and 5'-GTG CTG AGC CCT TCT GAA TC-3'; mKLF4, 5'-CAC CTG GCG AGT CTG ACA T-3' and 5'-TTC CTC ACG CCA ACG GTT A-3'; mCXCR4, 5'-AGC TAA GGA GCA TGA CGG AC-3' and 5'-TCC CAA AGT ACC AGT CAG CC-3'; mSOX2, 5'-AAA CTA ATC ACA ACA ATC GCG G-3' and 5'-GAT CTG GCG GAG AAT AGT TGG-3' ; mGAPDH, 5'-GCG AGA CCC CAC TAA CAT CA-3' and 5'-GAGTTGGGATAGGGCCTCTCTT-3'. Results were analyzed using StepONE (Applied Biosystems) and Excel (Microsoft) software and interpreted as %GAPDH in reference to each sample.

### **Immunohistochemistry Analysis**

Immunohistochemistry was conducted by the IU Pathology IHC Core Laboratory. Mouse lymph node tissue along with the surrounding fat was excised and immediately placed in paraformaldehyde for fixation. After fixation, the tissue block was embedded in paraffin and sliced with a microtome to approximately 5um thickness and fixed to slides for staining. PCK,  $\alpha$ -SMA, and Ly51 antibodies were used with varying secondary antibodies according to Pathology IHC Core titrations of antibody.

### **Immunofluorescent Microscopy Analysis**

Immunofluorescence was conducted using fresh and cultured mouse EpCAM<sup>+</sup> cells. Antibodies were diluted at 1:100 of the tube volume with a minimum of 1  $\mu$ L of antibody and 100  $\mu$ L of FACS buffer for every 1e6 cells. Antibodies were incubated at 4°C for 30 minutes and subsequently washed two times with FACS buffer and centrifuged for 5 minutes at 350RPM. Cells were then placed into Lab-Tek 8 well Glass Chamber Slides (Thermo, Rochester, NY) for viewing on the Olympus 2 confocal microscope located in the Indiana Center for Biological Microscopy, Division of Nephrology, IUSM. 4',6-Diamidino-2-Phenylindole, Dihydrochloride (DAPI) (Life technologies, Carlsbad, CA) was used for nuclear staining of all cells at a concentration of 3  $\mu$ M and an incubation of 15 minutes at room temperature. DAPI visualization was collected using Laser 405 with a voltage of 450 kV and an 8% laser. PCK (Mouse, IgG1, Alexa Fluor-488, clone AE1/AE3) and gp38 (Hamster, IgG, Alexa Fluor-488) were collected using Laser 488 with a voltage of 750 kV and a 10% laser. EpCAM (Rat, IgG2a, APC, clone test2) was collected using Laser 647 with a voltage of 8%. Images were collected and combined using a 60x lens and imaging software ImageJ (National Institute of Health.)

### **ELISAs**

Supernatant was collected from co-culture experiments and frozen or freshly analyzed using the mouse IFN $\gamma$  and IL-6 Quantikine ELISA kits (R&D Systems, Minneapolis, MN). ELISAs were conducted using the protocol described by the manufacturer.

### **Primary Culture of Unique Mouse Populations**

Multiple techniques were used to grow primary cultures of mouse populations. The first condition attempted was complete RPMI with 10 %FBS in 6 well plates. Further attempts to

grow the EpCAM+ population included using DMEM with 10% FBS in 6 well plates. Further attempts included using irradiated (4000 rads) NIH fibroblast 3T3s from the American Type Culture Collection (ATCC) as feeder cells to provide growth factors and a niche for the epithelial cell growth. Successful cultures of EpCAM+ cells used LA7 rat tumor mammary epithelial cell purchased from ATCC (CRL 2283) irradiated at 6000 rads and plated at concentrations of  $1.04 \times 10^5$  cells/cm<sup>2</sup> in six-well plates. LA7 cells were maintained using DMEM media with 10 ug/mL insulin, 50nM hydrocortisone, and 5% FBS. For growth of EpCAM+ cells the paper concerning rodent mammary epithelial cell growth according to Ehmann et al. 2003 was used [56]. EpCAM+ growth on LA7's was conducted using DMEM/Ham's F12 1:1 ratio supplemented with 10ug/mL insulin, 5ug/mL transferrin, 10% FBS, and 20mM HEPES.

## Results

### **Introductory phenotypic analysis of mouse EpCAM+ cells and Ly51+ cells by flow cytometry**

In order to better understand the role that the EpCAM+ and Ly51+ cells play in the immune system, a full analysis of surface and internal markers was conducted. This analysis gave us further insight into the origin and possible function of the cells of interest. Initial analysis consisted of the canonical markers for endothelium and epithelium,  $\alpha$ -smooth muscle actin (SMA) and pan-cytokeratin (PCK) respectively (Figure 6). The Ly51+ cell population is  $\alpha$ -smooth muscle actin positive ( $\alpha$ -SMA) which is characteristic of endothelial cells [57] and the Ly51+ MHCII+ cell population is LYVE-1+ which is characteristic of lymphatic endothelial cells [58]. The EpCAM+ population is entirely pan-cytokeratin (PCK) positive which is characteristic of epithelial cells [59]. The EpCAM+ population can be further subdivided into two distinct populations: gp38+ cells and gp38- cells.

### **Phenotypic analysis of mouse EpCAM+ cells by confocal immunofluorescent microscopy**

Immunofluorescence (IF) studies also demonstrate the PCK positivity of EpCAM+ cells (Figure 7). Analysis using confocal IF shows that approximately 50% of the EpCAM+ cells are gp38+, coinciding with the flow cytometry data. Gp38 is a marker for lymphatic endothelium and fibroblastic reticular cells. This data helps to further characterize the EpCAM+ cell population as epithelial in origin, while the  $\alpha$ -SMA+ Ly51 + population exhibits the phenotype of a lymphatic endothelial cell.

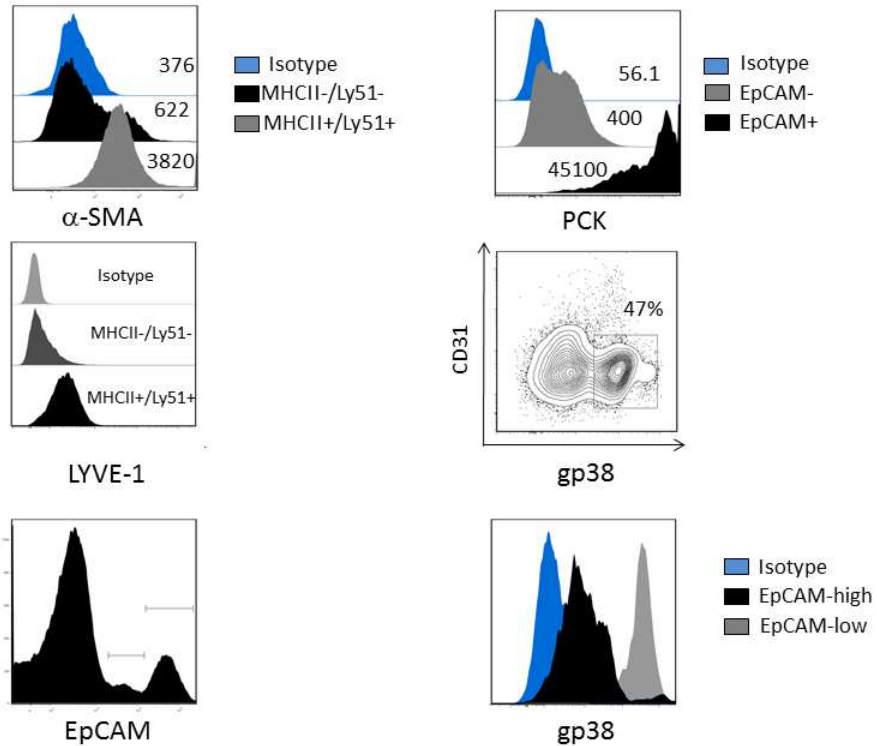


**Fig 6. Introductory descriptive analysis of Ly51+ and EpCAM+ cells.** The Ly51+ cell population is  $\alpha$ -smooth muscle actin positive ( $\alpha$ -SMA) which is characteristic of endothelial cells [57] and LYVE-1+ which is characteristic of lymphatic endothelial cells [58]. The Ly51+ population consists of two populations: MHCII+ and MHCII-. The EpCAM+ population is entirely pan-cytokeratin (PCK) positive which is characteristic of epithelial cells [59]. The EpCAM+ population can be subdivided into two distinct populations: gp38+ cells and gp38- cells. These two EpCAM+ populations will be analyzed in order to determine the individual cell population functions. EpCAM low populations express high gp38, while EpCAM high populations express little gp38. Figures shown are representative of n=3 independent experiments with equivalent biological results.



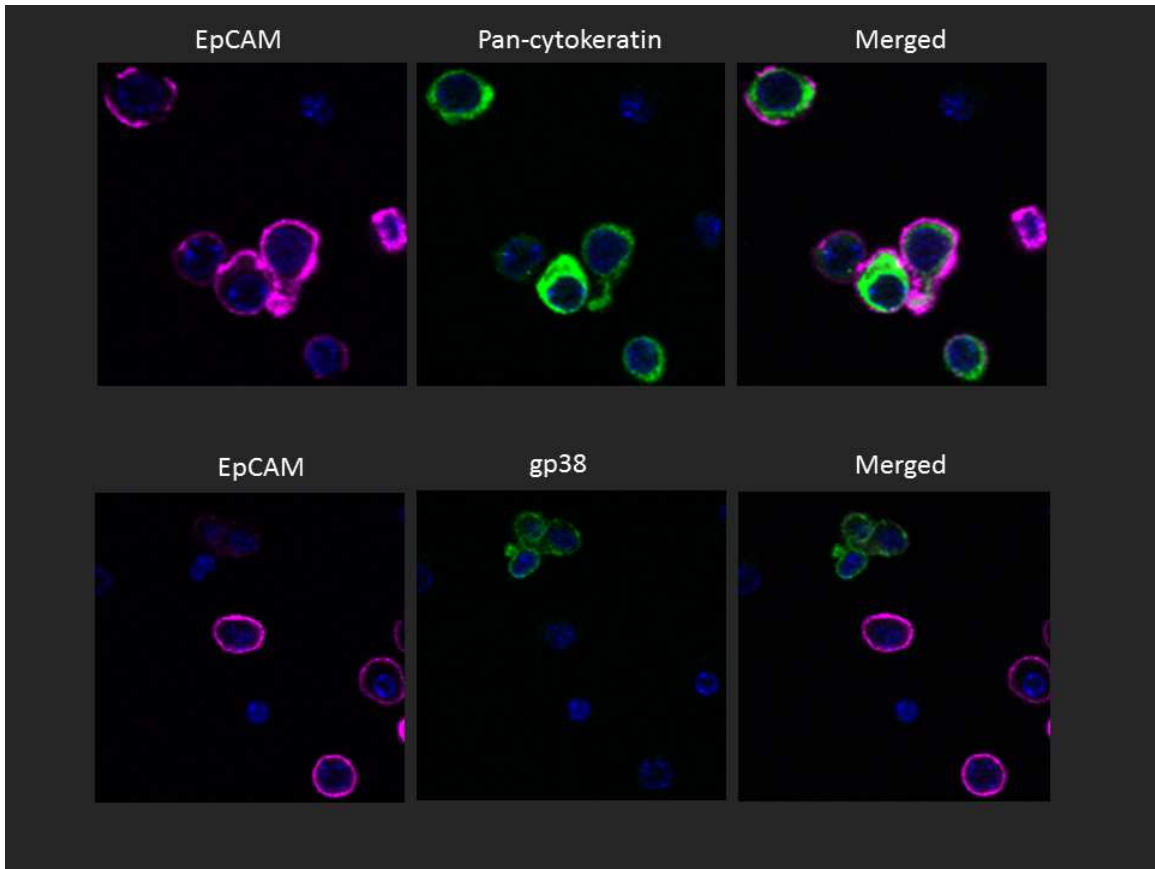


**Fig 7. Immunofluorescent microscopy of freshly isolated EpCAM+ cells.** The immunofluorescence reinforces the previous flow cytometry findings of an entirely PCK+ EpCAM population. It also demonstrates that approximately 50% of the EpCAM+ cells are gp38-, while the other 50% are gp38+. Again, cells that stain dimly for EpCAM, stain strongly for gp38 while cells that stain strongly for EpCAM have little to no gp38 expression.

### **Location of the EpCAM+ and Ly51+ population based on immunohistochemistry**

With a basic understanding of the origin and type of stromal cells we have isolated, the next focus was the location of the cells in respect to each other and the follicle. The lymph node of a mouse and the surrounding fat pads show distinct channels formed by  $\alpha$ -SMA+ cells and PCK+ cells (Figure 8). Further analysis depicts a smooth muscle actin positive population closely associating with the PCK+ population of epithelial cells. The channels consist of an epithelial (PCK+) cell population forming the luminal surface, while the smooth muscle cells form the exterior of the channel.

### **Detailed surface profile of EpCAM+ cells**

To better elicit the role of EpCAM+ cells in the lymph node and surrounding cells, a more robust surface marker profile study was conducted using flow cytometry. The analysis helped clearly define the population, gave hints at possible growth conditions based on growth factor receptors, and supplied us with possible avenues of functional studies. The first array of surface marker antibodies used included common indicators of cell adhesion and co-stimulation (Figure 9). Flow cytometric analysis demonstrates that the CD45-/EpCAM+ population's cell surface has medium levels of CD40, CD86, and PDL1 and high levels of LtBR on their surface. CD40 is a co-stimulatory molecule found on APCs and is required for activation of APCs by binding CD154 on T helper cells inducing stimulation of T helper cells and APCs [60]. CD54 is a glycoprotein expressed on endothelial cells, and when ligated can cause downstream inflammatory effects and leukocyte recruitment [61]. CD80 and CD86 are co-stimulatory signals for T cell activation and survival and act by ligating CD28 and CTLA4 on the surface of T cells [62]. CD106 is a cell adhesion molecule commonly found on stimulated blood vessels that mediates the adhesion of leukocytes [63].

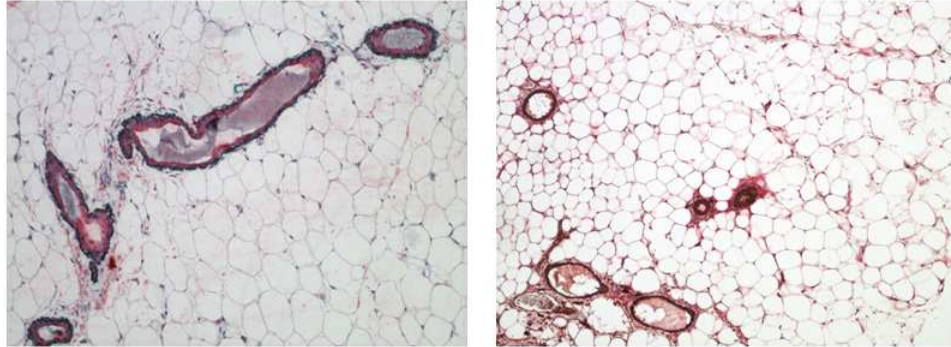


**Fig 8. Histological microscopy of the fat pad surrounding the inguinal lymph node follicle in BL/6J mice.** In order to elicit the location of the EpCAM+ and Ly51+ populations histological staining of mouse lymph node fat pads was conducted. **Left Pane:** 200x.  $\alpha$ -SMA-green, PCK-red. **Right Pane:** 200x. Ly51-Red, PCK-brown. Surrogate markers  $\alpha$ -SMA and PCK were used for Ly51 and EpCAM respectively due to poor staining by the Ly51 and EpCAM antibodies. Seen above are channels formed with the epithelial cells forming the luminal surface, while the smooth muscle cells form the exterior of the channel.

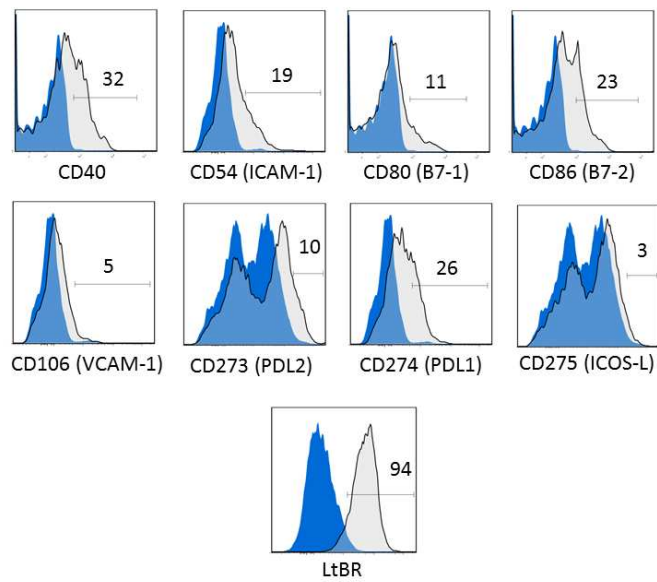


**Fig 9. Flow cytometric analysis of CD45-/EpCAM+ cell surface markers (adhesion and costimulation).** Isotypes corresponding to each constant region, species, and fluorophore were used for each analysis. Numbers indicate percent of mean fluorescent intensity (MFI) above the isotype control. Figures shown are representative of n=3 independent experiments with equivalent biological results.

PDL1 and PDL2 play role in suppressing the immune system by interacting with PD-1 on the surface of CD8+ cytotoxic T cells; therefore, inhibiting proliferation [64-66]. CD275 is present on APCs and binds ICOS on activated T cells for co-stimulation [67]. LtBR plays a role in lymph node development and we hypothesize that it may suppress T cells through an unknown mechanism: possibly through the iNOS or IDO1 pathway or by up-regulating PDL1 [34, 35].

Further analysis on the CD45- EpCAM+ population of lymph node and surrounding tissue stroma was focused on the mesenchymal and stem-like properties of the unique cell population (Figure 10). Analysis of common stem-like markers demonstrated that the EpCAM+ population express medium levels of CD38, CD44, CD140a, CXCR4, OCT4, Sca-1, CD9, and CD29 eliciting a possible multi-potency potential of the cell population. CD38 is widely expressed on many tissues, can bind CD31, and can mediate lymphocyte activation and adhesion [68]. CD44 is expressed on some epithelial cells and is a receptor for hyaluronic acid [69]. CD140a is expressed on mesenchymal-derived cells of adult mouse tissue [70]. CD157 is present on bone marrow stromal cells and plays a role in pre-B-cell growth [71]. CXCR4 is commonly found on hematopoietic stem cells (HSCs) and lymphocytes and binds SDF-1 (CXCL12) present on BM stromal cells [72]. Oct4, a transcription factor, is commonly used as a marker for undifferentiated tissue [73]. Sca-1 and c-kit are HSC markers and are present on some endothelial cells [74]. CD9 and CD29 are both possible marker for stem-like cells [75, 76]. MHC I is positive as to be expected with any nucleated cell. In total, the flow cytometric analysis gives an indication of the possible origin, stem-like, and adhesive properties of the EpCAM+ cell population.

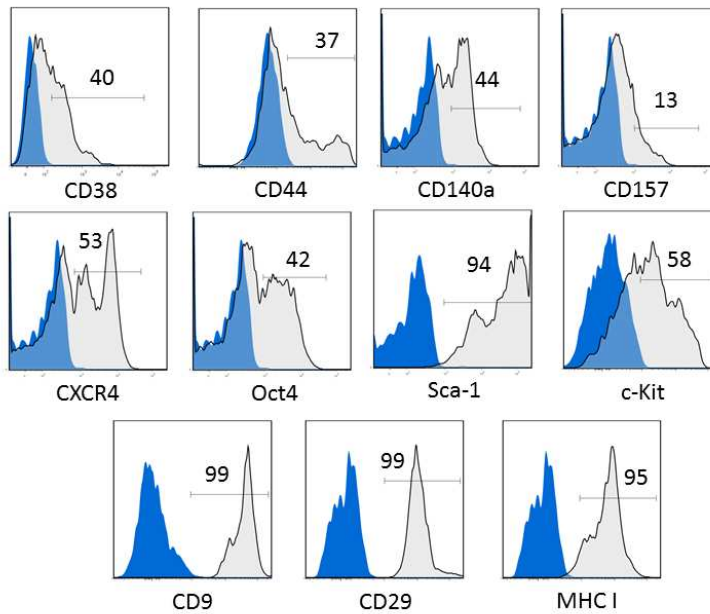


**Fig 10. Flow cytometric analysis of CD45-/EpCAM+ cell markers [stem-like, MSC-like (mesenchymal stem cell), and miscellaneous].** Isotypes corresponding to each constant region, species, and fluorophore were used for each analysis. Numbers indicate percent of mean fluorescent intensity (MFI) above the isotype control. Figures shown are representative of n=3 independent experiments with equivalent biological results.

### **Growth attempts of CD45- EpCAM+ cells**

In order to further study the EpCAM+ cells we decided to initiate primary cultures. This would allow us to accomplish several things: 1) Identify the similarities between freshly isolated and cultured EpCAM+ cells. 2) Eliminate the need for time and resource draining fresh mouse preparations. 3) Utilize large quantities of grown EpCAM+ cells for co-culture experiments with T cells. 4) Establish a long lasting cell line for further studies in the future.

Initial attempts to grow the EpCAM+ cells consisted of placing the sorted EpCAM+ cells into media containing RPMI with 10% FBS. Growth was slow and insufficient number of cells for desired experiments resulted (Figure 11). The next step in growth attempts included using irradiated 3T3 fibroblasts as feeder cells to support the EpCAM+ cells in adhesion and growth. This more successful method of culturing resulted in faster growth. Further analysis of grown EpCAM+ cells in RPMI with irradiated 3T3s demonstrated the retention of a similar surface profile to freshly isolated EpCAM+ cells. The cultured EpCAM+ cells retained the 1:1 ratio of gp38+ and gp38- cells seen in flow cytometry and immunofluorescent analysis (Figure 12). In attempt to replicate the successful mammary epithelial cell growth conducted by Ehmann et al [56], irradiated LA7 cells were used with media consisting of DMEM/Ham's F12 1:1 ratio supplemented with insulin and transferrin. This resulted in successful growth of EpCAM+ cells, but instead of the characteristic 1:1 ratio of gp38+ to gp38- cells, only gp38- cells were found (Figure 13). This may be due to the depletion of EpCAM<sup>LOW</sup> gp38+ cells during magnetic column selection.

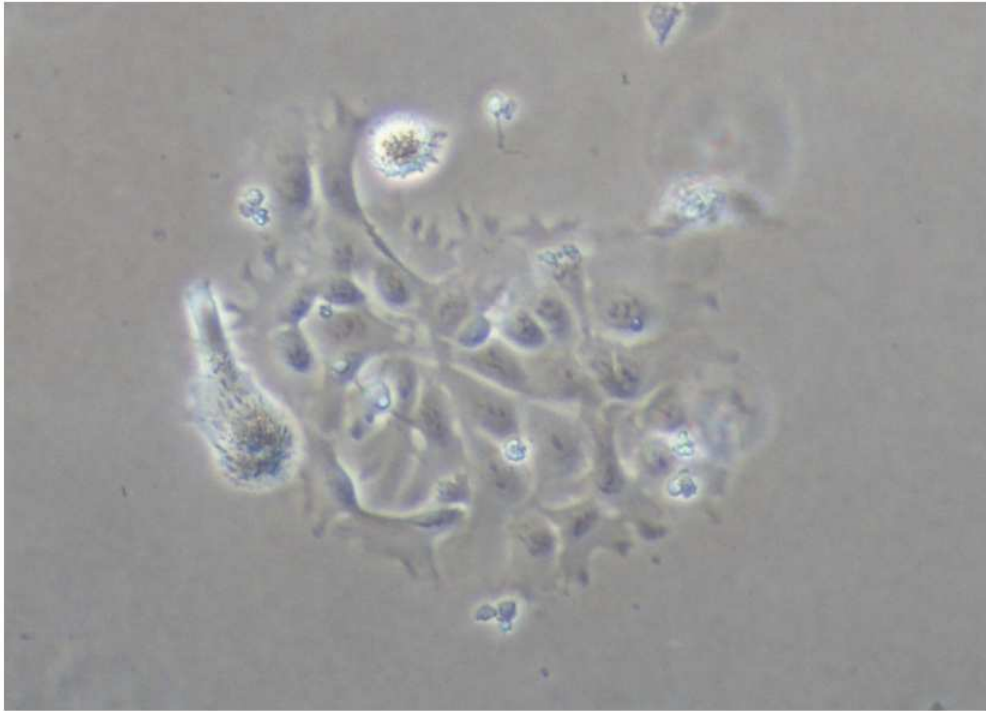


**Fig 11. Day 4 culture of EpCAM+ cells in RPMI 10% FBS.** A colony of EpCAM+ cells is seen growing in the above picture.



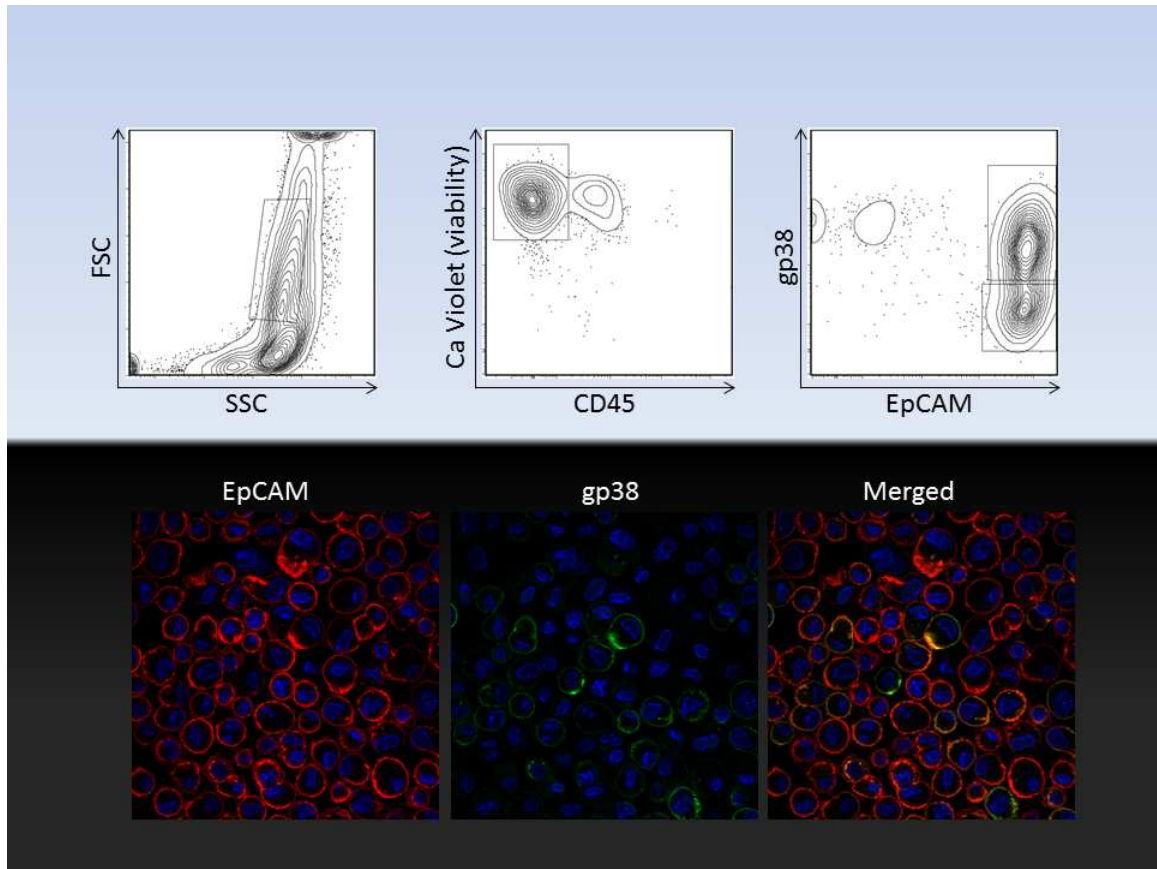


**Fig 12. Day 12 growth of EpCAM+ cells on irradiated 3T3's increases growth potential.** Further attempts to grow EpCAM+ cells resulted in greater success. Lymph node follicles and the surrounding fat were collected, digested with collagenase, RBC lysed, CD45+ cell depleted, Ly51 depleted, and finally positively selected for EpCAM+ cells using magnetic separation. EpCAM+ cells were plated at a concentration of  $1.04 \times 10^4$  cells/cm<sup>2</sup> on a bed of 4000 rad irradiated 3T3 fibroblasts at a concentration of  $1.6 \times 10^3$  cells/cm<sup>2</sup> in 6 well plates. Media used was DMEM with 10% FBS. Cells harvested on day 12 demonstrated EpCAM positivity by flow and immunofluorescence. Cells also demonstrated the consistent 50% gp38+ population and 50% gp38- population.

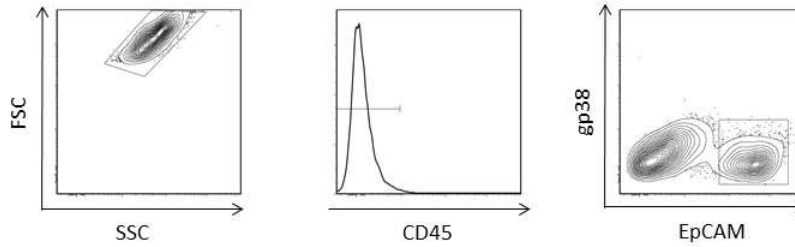
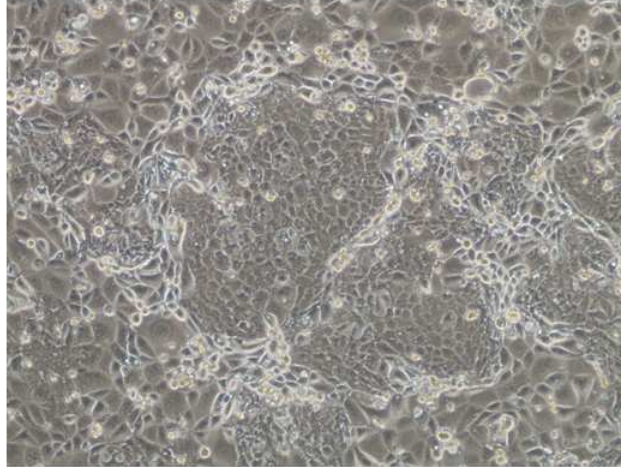


**Fig 13. 8 Day growth of EpCAM+ cells plated on confluent, irradiated LA7 rat mammary cells.**

$1.04 \times 10^5$  LA7 cells/cm<sup>2</sup> were irradiated at 6000 rads and plated 24 hours prior to plating  $1.04 \times 10^4$  EpCAM+ cells. The smaller, rounder EpCAM+ cells can be seen pushing the LA7 cells outwards as growth of EpCAM+ cells replaces the irradiated LA7s. Flow cytometric analysis shows an EpCAM+ population with no gp38 positivity.

### **Ly51+ stromal cells uptake exogenous antigen and cross-present to CD8 T cells.**

To better understand the role the EpCAM+ cells were playing around the lymph node, the other unique population, Ly51+ cells, was analyzed for its role in antigen presentation and T cell stimulation. The normal pathway for exogenous antigen after endocytosis results in presentation on MHC-II. Ly51+ cells are capable of up-taking exogenous antigen resulting in cross-presentation of antigen in the context of MHC-I. This leads to CD8 T cell activation, down-regulation of CD25 (IL-2 receptor), and up-regulation of T cell early activation marker CD69. Proliferation is evident from the CFSE studies shown. Compared to dendritic cells (DCs) Ly51+ cells result in less IFN $\gamma$  production by T cells. IL-6 is constitutively produced by Ly51+ cells (Figure 14).

### **The inhibitory effects of EpCAM+ cells on T cells**

The proliferative effect Ly51+ cells have on T cells may be counterbalanced by the inhibitory effect of the adjacent EpCAM+ cells. Varying amounts of EpCAM+ cells had a dose dependent inhibition of bead-activated T cell activation and proliferation (Figure 15). With increasing amounts of EpCAM+ cells co-cultured with fixed numbers of T cells, one sees the inhibitory effect of EpCAM+ cells keeping T cells in their non-activated (CD44- CD62L+) naïve state (Figure 16). EpCAM+ lymph node stromal cells are also found to inhibit the production of IL-2 in a dose dependent manner especially when compared to the total CD45- population which contains the stimulatory Ly51+ cells and the inhibitory EpCAM+ cells. When the EpCAM+ cells are isolated and interacting with activated T cells, production of IL-2 drops. IL-6 is produced by both the EpCAM+ population and the entire CD45- population in similar amounts (Figure 17).

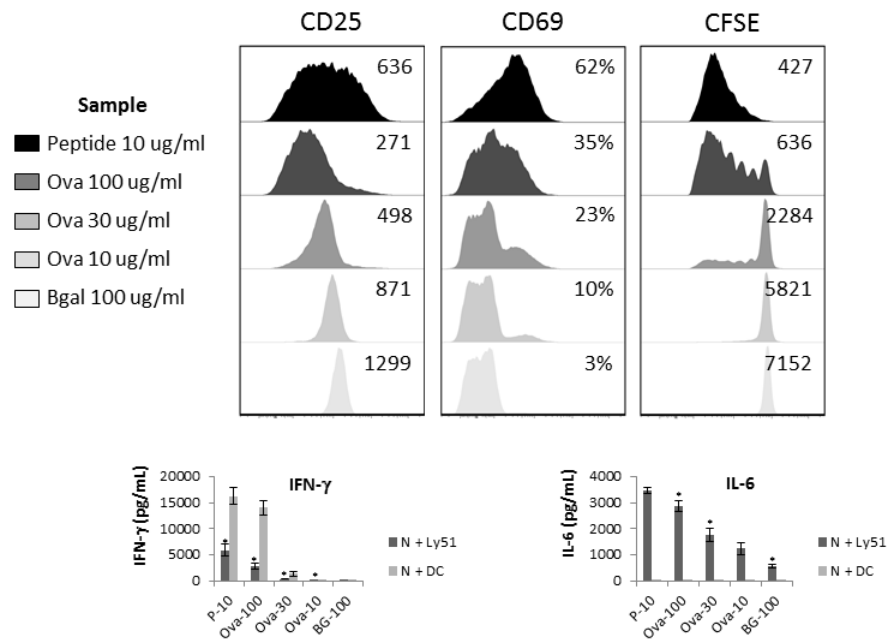


**Fig 14. Ly51+ lymph node stromal cells can uptake Ova and cross-present to naïve OT-I T cells.**

3 day co-culture of Ly51+ lymph node stroma with OT-I T cells presented with antigen by CD11c+ dendritic cells. The flow cytometry is of the day 3 OT-I T cells while the ELISA data located in the bottom two panels is from the supernatant collected on day 3 of the co-culture. OT-I T cells contain TCRs specific for ova peptide in the context of MHC-I. T cells produce IFN- $\gamma$  when activated [77]. CFSE is a measure of proliferation, with the smaller the mean fluorescence intensity (MFI), the more proliferation occurs [78]. Numbers in CD25 and CFSE flow histograms indicate MFI. Percentages in CD69 indicate MFI percentage above isotype. Statistical significance was calculated using ANOVA ( $p < .05$ ) followed by post-hoc student's T test. \* indicates significant differences between groups ( $p < .05$ ).  $n=3$  for sample analysis. Data shown is representative of 3 independent experiments with equivalent biological end results.

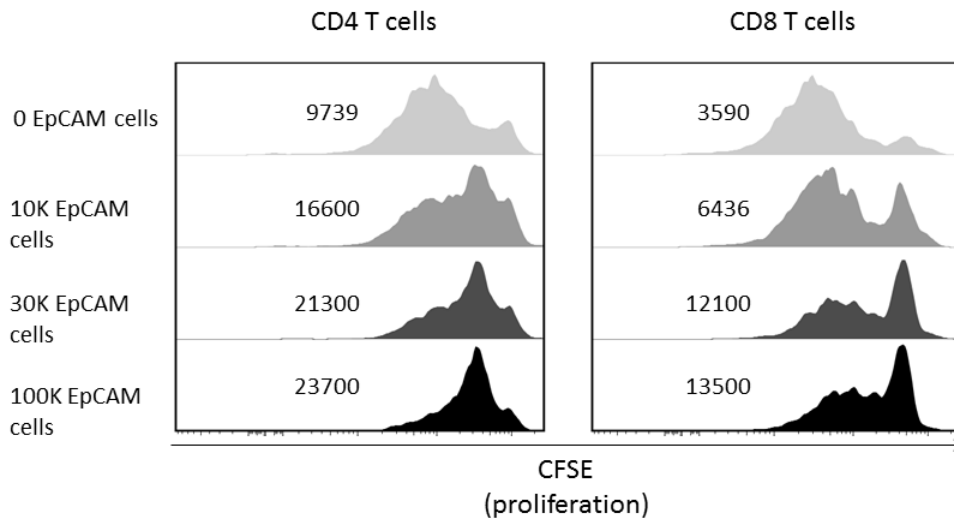


**Fig 15. EpCAM+ cells demonstrate the ability to inhibit the proliferation of bead-activated CD4 and CD8 T cells in a dose-dependent manner.** 3 day co-culture of passage 0 (P0) cultured EpCAM+ lymph node stromal cells with CD3/CD28/CD137 bead activated CD4 and CD8 T cells in a 96 well U-bottom plate. The mean fluorescence intensity of CFSE correlates with the reverse amount of proliferation: the less CFSE present in flow cytometry, the more proliferation occurred. With the addition of  $1 \times 10^5$  EpCAM+ cells, one sees a marked decrease in the proliferation of activated CD4 and CD8 T cells. Numbers in histograms indicate the MFI. Figures shown are representative of 2 independent experiments with biologically equivalent results.

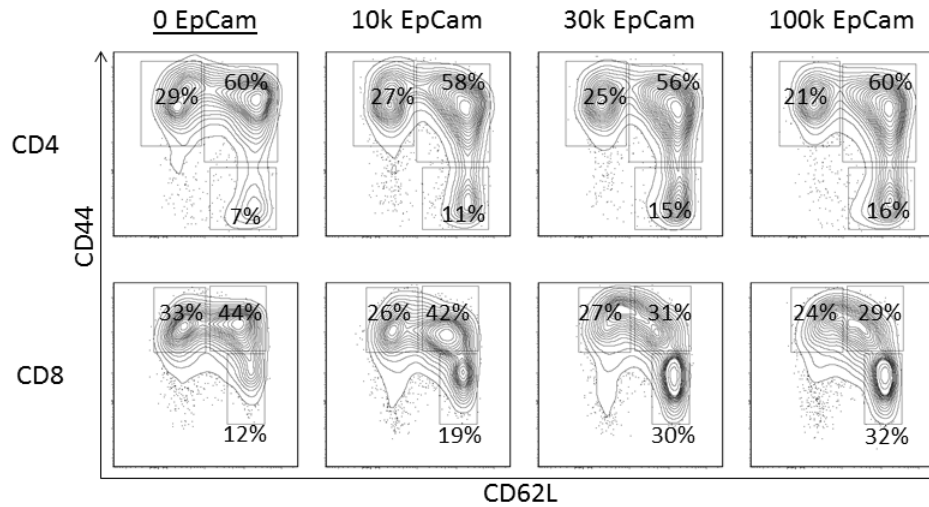


**Fig 16. EpCAM+ cells can keep bead-activated T cells in their naïve state.** Passage 0 cultured EpCAM+ lymph node stromal cells were capable of retaining the activated CD4 and CD8 T cells in their naïve CD44- CD62L+ state in a dose-dependent manner in a 3 day co-culture in U-bottom 96 well plates. CD44+ CD62L- T cells are effector T cells while CD44+ CD62L+ T cells are memory T cells [79]. Results shown are representative of 2 independent experiments with equivalent biological results.

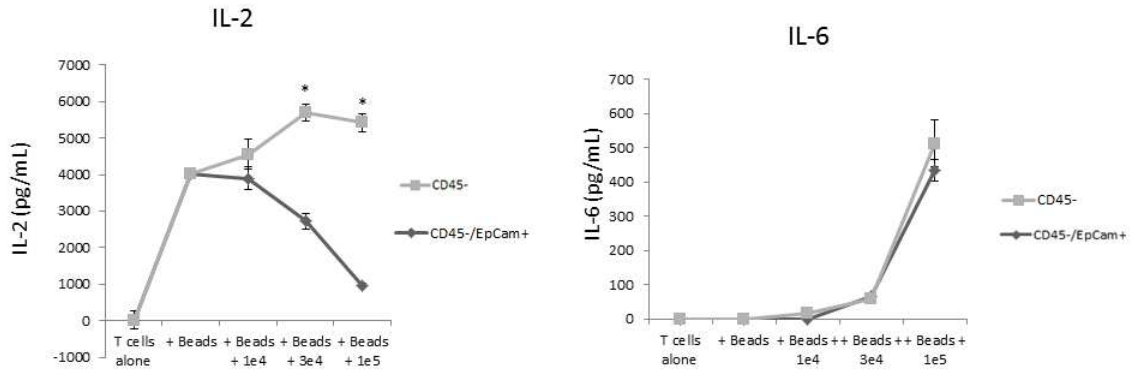


**Fig 17. EpCAM+ lymph node stromal cells inhibit the production of IL-2 in a dose dependent manner.** 3 day co-culture of bead-activated T cells with either CD45- stroma (containing Ly51+ and EpCAM+ T cells) or CD45- EpCAM+ stroma alone demonstrates that EpCAM+ cells can inhibit the production of IL-2, an essential cytokine for T cell proliferation [80]. IL-6 is produced equivalently by both the CD45- population and the isolated EpCAM+ population. Statistical analysis between the EpCAM+ group and the CD45- group was conducted using ANOVA ( $p < .05$ ) followed by post-hoc student T tests between each group at each concentration of cells. \* indicates significant difference ( $p < .05$ ).

### **Contact-mediated and secretory actions of EpCAM+ inhibition on activated T cells.**

Transwell and U-bottom plates were used to elicit the role secreted factors and direct contact could be playing in T cell inhibition. Based on MFIs, EpCAM+ stromal cells moderately inhibit the proliferation of T cells through a secreted mechanism, but exhibit even stronger inhibition in a contact-mediated setting as shown in the U-bottom plate. Down-regulation of CD25, the IL-2 receptor, also demonstrates the inhibitory potential of EpCAM+ lymph node stromal cells in both a secretory system and a contact-mediated system (Figure 18).

### **IDO1 and iNOS: possible mechanisms of T cell inhibition by EpCAM+ lymph node stromal cells.**

qPCR analysis of co-cultured EpCAM+ cells with T cells that were activated with either beads or APCs presenting specific antigen resulted in up-regulation of the genes IDO1 and iNOS. When EpCAM+ cells encounter secreted factors from activated T cells, IDO and iNOS are up-regulated (Figure 19).



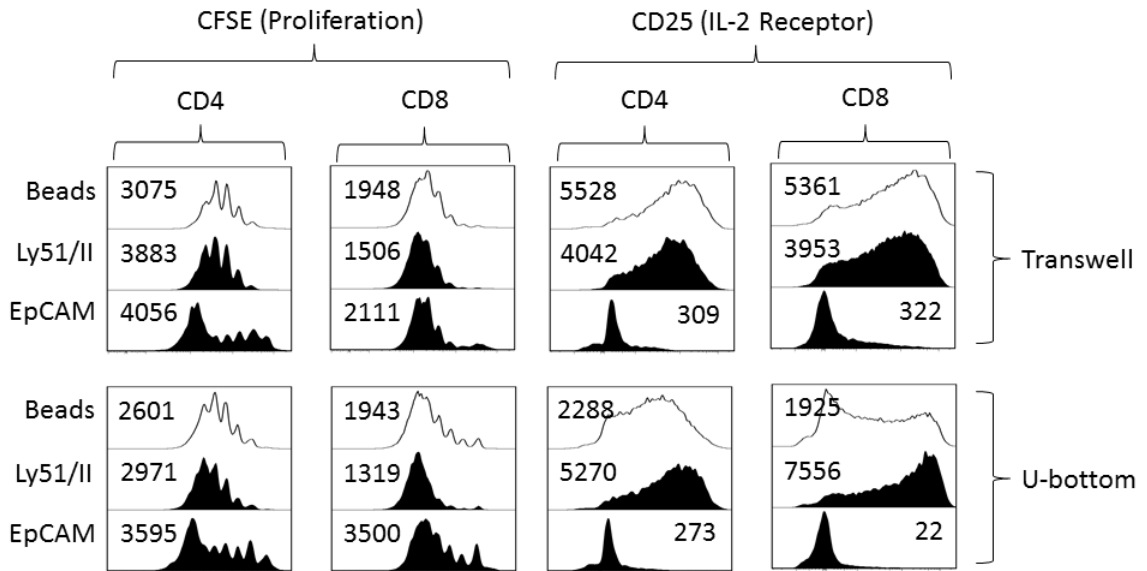


**Fig 18. Inhibition of T cells by EpCAM+ lymph node stroma: contact mediated or secretion-dependent.** A 3 day co-culture of either EpCAM+ stromal cells or Ly51+MHCII+ stromal cells with bead activated CD4 or CD8 T cells in either a contact-mediated environment (U-bottom) or secretion-dependent system (transwell) is shown above. Numbers in histograms indicate MFI. Results shown are representative of 2 independent experiments with equivalent biological end results.

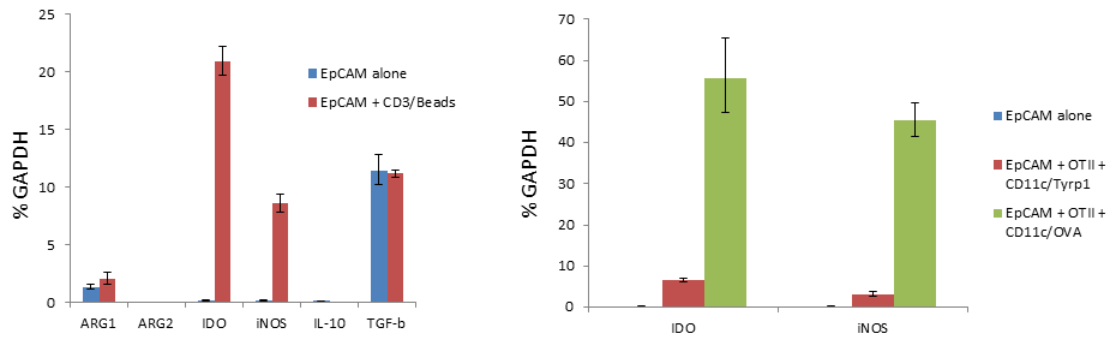


**Fig 19. EpCAM+ cells up-regulate potential T cell inhibitory genes IDO and iNOS in response to secreted factors released by bead-activated T cells.** Gene expression was analyzed using %GAPDH. The left panel shows a 36 hour co-culture of EpCAM+ cells with Bead activated CD3 T cells in transwell 96 well plates. The right panel shows a 72 hour transwell EpCAM+ cell co-culture with OT-II T cells stimulated by CD11c+ dendritic cells presenting the OT-II specific protein, ova, or a control protein, Tyrp1, that should not stimulate OT-II T cell activation. Each graph is representative of n=1 patient with samples analyzed in triplicate.

## CHAPTER 2. HUMAN LYMPH NODE STROMA

### **Introduction**

Human lymph node stroma cell populations were isolated to identify populations that may be analogous to our mouse model populations: EpCAM+ and Ly51+MHCII+. The unique ability to resect and begin preparation of human lymph nodes immediately following surgery has given us the opportunity to analyze the distinct populations before cell death occurs. Freshly resected human lymph nodes were analyzed based on two primary markers: CD34 and HLA-DR. CD34 is present in all Ly51+ lymph node cells in our mouse studies and represents a sufficient surrogate marker for Ly51 and endothelial cells in general. HLA-DR is the human form of the MHCII complex. There is insufficient evidence of any epithelial cell populations that may be analogous to the mouse EpCAM+ population. The main goal of the human lymph node studies was to characterize the cell populations using surface marker expression, internal markers, and gene expression assays in order to determine further courses of action regarding the function of the cells.

## **Materials and Methods:**

### **Lymph Node Collection**

Lymph nodes were collected from healthy patients undergoing limb reperfusion and immediately placed in saline on ice. All tissue harvests were conducted according to institutional review board (IRB) regulations. Human lymph nodes were procured from healthy donors (fresh) and were never frozen. The tissue was digested, processed, and analyzed within 5 hours of collection. Lymph nodes and the surrounding fat pads were excised and directly placed in saline solution and placed on ice.

### **Preparation of Lymph Node**

Tissue was kept on ice unless otherwise indicated. Tissues from individual human patients were separated based on fat and lymph node. Lymph nodes were then cut into smaller 10mm sections using forceps and a scalpel. Lymph nodes were further mechanically processed by holding the 10mm sections in place and crushing the tissue with the butt end of a 10mL syringe plunger. Tissue was then placed into GentleMACS C tubes (approximately 6 grams/C tube) (Miltenyi Biotec Inc., Auburn, CA) containing 3 mL of cold Hyclone RPMI (Thermo Scientific, Waltham, MA) supplemented with 10% Hyclone FBS, 100 I.U./mL Penicillin, 100 ug/mL Streptomycin, 1mM Sodium Pyruvate, 1x MEM Nonessential Amino Acids ((Mediatech, Manassas, VA), 2mM L-Glutamine, 20mM HEPES (Lonza, Walkersville, MD), and 1x 2-Mercaptoethanol (Gibco, Grand Island, NY) and dissociated using the GentleMACS Dissociator (Miltenyi Biotec Inc.) on default setting "spleen 02" (14 seconds). Any tissue remaining in the blades of the GentleMACS C tube was removed using forceps and placed into the remaining dissociated tissue. 10 ug Collagenase D (Roche, Basel, Switzerland) was dissolved in 2mL of

supplemented RPMI and added to the 3 mL of RPMI containing the dissociated tissue for a final w/v of 0.2%. Lymph node tissue was incubated at 37°C (5% CO<sub>2</sub>) for 30 minutes, and then dissociated for 60 seconds with the GentleMACS Dissociator default setting “Spleen 01”, again incubated for 30 minutes at 37°C, and finally dissociated again for 60 seconds using the “Spleen 01” setting. 45 mL of supplemented RPMI added to digested lymph node and transferred to a 50 mL conical tube and centrifuged at 400 RPM for 10 minutes. Supernatant was disposed (no cells present in supernatant) and pellet was re-suspended in 2 mL of 1x RBC Lysis Buffer (eBioscience) for 60 seconds and inactivated with 30 mL cold FACS buffer (2% FBS in Thermo Scientific PBS.) Suspension then filtered through a 40 um cell strainer (Thermo Scientific) and strainer rinsed with an additional 20 mL of FACS buffer. Cell suspension centrifuged at 350 RPM for 5 minutes and resuspended in FACS buffer for flow cytometric analysis or supplemented RPMI for growth studies or selected for CD45- cell populations using CD45 MicroBeads (Miltenyi Biotec, Bergisch Gladbach, Germany.) CD45 microbeads were added to the disaggregated cell populations, incubated at 4°C for 30 minutes, followed by 2 washes with MACS buffer and then a run through an LS column attached to a magnet and magnetic stand (Miltenyi Biotec.) Run through was collected and analyzed with flow cytometry, qPCR, or chosen for growth and differentiation studies.

### **Flow Cytometry Analysis**

Antibodies were purchased from eBioscience (San Diego, CA) unless otherwise noted. Events were collected with the LSRII flow cytometer (BD Biosciences) at IUSM’s Flow Cytometry Core. Antibodies were diluted at 1:100 of the tube volume with a minimum of 1uL of antibody and 100 uL of FACS buffer for every 1e6 cells. Antibodies were incubated at 4°C for 30 minutes and subsequently washed two times with FACS buffer and centrifuged for 5 minutes at 350RPM.

Analysis was performed using FlowJo (Tree Star Inc., Ashland, OR.) Isotype controls and compensation controls used for every analysis. CellTrace™ Calcein Violet, AM (Invitrogen, Carlsbad, California), diluted 1:1000 used for cell viability. Intracellular staining was conducted using eBioscience intracellular staining protocol A with IC Fixation Buffer and Permeabilization Buffer. CellTrace Carboxyfluorescein succinimidyl ester (CFSE) Proliferation Kit (Molecular Probes, Eugene, Oregon) was used for proliferation quantification. Cell sorting was conducted using the BD FACSaria (BD Biosciences) located at IUSM’s Flow Cytometry Core. List of antibodies used (Figure 20).

Epitope	Species	Isotype	Fluorophore	Clone
CD105	Mouse	IgG1	APC	SN6
CD106	Mouse	IgG1	APC	STA
CD123	Mouse	IgG1	APC	6H6
CD144	Mouse	IgG1	APC	16B1
CD146	Mouse	IgG2a	APC	MUC18, Mel-CAM
CD19	Mouse	IgG1	APC-eF780	HIB19
CD31	Mouse	IgG1	APC	WM59
CD34	Mouse	IgG1	APC	4H11
CD34	Mouse	IgG1	FITC	4H11
CD44	Rat	IgG2b	APC	IM7
CD45	Mouse	IgG1	PE	HI30
CD45	Mouse	IgG1	APC	HI30
CD45	Mouse	IgG1	PE-Cy7	HI30
CD73	Mouse	IgG1	APC	AD2
CD90	Mouse	IgG1	APC	5E10
CXCR5	Mouse	IgG2b	PE	MU5UBEE
DLL-1	Mouse	IgG1	PE	MHD1-314
gp38	Rat	IgG2a	APC	NZ-1.3
HLA-ABC	Mouse	IgG2a	APC	W6/32
HLA-DQ	Mouse	IgG1	FITC	SK10
HLA-DR	Mouse	IgG2a	PE	L243
HLA-DR	Mouse	IgG2a	FITC	L243 (G46-6)
LtBR	Mouse	IgG1	APC	71319
LYVE-1	Mouse	IgG1	APC	537028
SMA	Mouse	IgG2a	FITC	1A4
VEGFR3	Mouse	IgG1	APC	54733

**Fig 20. Antibodies used for human analysis**

## qRT-PCR Analysis

Quantitative real time PCR was performed using lymph nodes and surrounding tissues digested and prepared as described. Cells were sorted for CD45- Calcein Violet+/EpCAM+ and CD45- Calcein Violet+/Ly51+MHCII+. 200,000 cells were used for preparation of each RNA sample. RNA was prepared using RNeasy Plus Mini Kit to the manufacturers specifications (Qiagen, Venlo, Limburg.) Due to the limited amount of starting RNA, SMART mRNA Amplification Kit (Clontech, Mountain View, CA) was used to linearly amplify mRNA prior to reverse transcription. cDNA was reverse transcribed from isolated RNA using the High Capacity cDNA Reverse Transcription Kit (Invitrogen, Carlsbad, CA) according to the manufacturer's protocol. SYBR Green PCR Master Mix (Applied Biosystems, Foster City, CA) or TaqMan Real Time PCR Master Mixes (Life Technologies, Carlsbad, CA) were used for the qPCR reaction according to the manufacturer's protocol. Samples were run on the STEPOne PLUS Real Time qPCR System (Applied Biosystems). All primers were designed using PrimerBlast software (NIH) using the following requirements: PCR product size, 70-150; primer melting temperatures minimum, 58.0; optimum, 60.0; maximum, 60.0; maximum temperature melting difference, 2; exon should span an exon-exon junction; Guanine Cytosine (GC) content, 30-36; maximum polynucleotides, 3; maximum self-complementation, 5, 3 in a row; concentration of monovalent cations, 60; both primers need the same melting temperature [55]. The following 25 nmol oligonucleotide DNA primers were ordered from Integrated DNA Technologies: Results were analyzed using StepONE (Applied Biosystems) and Excel (Microsoft) software and interpreted as %GAPDH. Primers used: hCD40, 5'- AGT CGG CTT CTT CTC CAA TGT -3' and 5'- CTT TGG TCT CAC AGC TTG TCC -3'; hCD80, 5'- ATC TGA CGA GGG CAC ATA CG -3' and 5'- AGG TGT AGG GAA GTC AGC TTT -3'; hCD83, 5'- TTG AGA GTG ACA GGA TGC CC -3' and 5'- AGA TAC TCT GTA GCC GTG CAA -3'; hCD86, 5'- ACT AGC ACA GAC ACA CGG AT -3' and 5'- GAC TGA AGT TAG CAG AGA GCA G -3'; hCD275, 5'- ATG

TGG CAG CAA ACT TCA GC -3' and 5'- AGG CTG TTG TCC GTC TTA TTG A -3'; hCD274, 5'- TGG TCA  
 TCC CAG AAC TAC CTC -3' and 5'- TCA GTG CTA CAC CAA GGC AT -3'; hCCL19, 5'- GGT GCC TGC  
 TGT AGT GTT CAC C-3' and 5'- CGG CGC TTC ATC TTG GCT GA -3'; hCCL21, 5' – TCA CCC TCA GCT  
 CTG GCC TCT T -3' and 5'- TCC ATC ACT GCC TTG GGT CCT G -3'; hCXCL12, 5'-  
 TGTGCCCTTCAGATTGTAGCCCG – 3' and 5' – TCG AGT GGG TCT AGC GGA AAG T -3'; hIL6, 5' –  
 AGC CCA CCG GGA ACG AAA GA -3' and 5'- ACT GGA CCG AAG GCG CTT GT – 3'; hTGFB1, 5' –  
 TTG TGC GGC AGT GGT TGA GC – 3' and 5' – GGC CGG TAG TGA ACC CGT TGA T-3'; hIL10, 5'-TCC  
 GAG ATG CCT TCA GCA GAG T-3' and 5'-GCT TGG CAA CCC AGG TAAC CCT TA-3'; hGAPDH, 5'-  
 TGT TCG ACA GTC AGC CGC ATC T-3' and 5'-CGC CCA ATA CGA CCA AAT CCG T-3'; hACTB, 5'- TCC  
 TTC CTG GGC ATG GAG TCC T - 3' and 5'- TGC GGA TGT CCA CGT CAC ACT - 3'; hMITF, 5' – TGA  
 AGA GCA GCA GTT CCG CC -3' and 5'- TGC TGG CGT AGC AAG ATG CG - 3'; hAIRE, 5'-CCC GAG  
 GAC AAG TTT CAG GAG ACG-3' and 5'-TCC AGG ATG GCT GTG GAG TCC T-3'; hIL3, 5' - GCA CCC  
 ACG CGA CAT CCA AT - 3' and 5' - ACG AGC TGG ACG TTG GAC TCA - 3'; hKITLG, 5'-AGT CCT GAG  
 AAA GGG AAG GCC AAA-3' and 5'-TGC CCT TGT AAG ACT TGG CTG TCT-3'; hFLT3LG, 5'-ACT TTC  
 GGT CTC TGG CTG TCA CC-3' and 5'-GAT AGG TTG TTG GGC TCC AGG CT-3'; hDLL1, 5'- GTC CGC  
 CGC TGT TCT AAG GAG A-3' and 5'-TCC AGA CCT GAC ACA GCA AGG C-3'; hIL7, 5'-TCC TGC TCC  
 AGT TGC GGT CA-3' and 5'-ACT GGC AAC AGA ACA AGG ATC AGG G-3'; hGMCSF, 5'-GCC AGC  
 CAC TAC AAG CAG CAC-3' and 5'-GCC TCA TCT GGC CGG TCT CA-3'; hIL3RA, 5'-GAT CTC CAT TTA  
 AGC AGG CAC C-3' and 5'-TAG GTT CGT GAT TGG TGG GTT-3'; hCCR1, 5'- TTG GAA CCA GAG AGA  
 AGC CG - 3' and 5'- CTC TCG TTC ACC TTC TGG CA - 3'; hCCR2, 5'- AGC CAC AAG CTG AAC AGA  
 GA - 3' and 5'- GGT GAC TTC TTC ACC GCT CT - 3'; hCCR3, 5'-TGA CGC CTA AGC TAT CAC TGG-3'  
 and 5'-TTG TCA TTT CAC TTC TCC CTG AA-3'; hCCR4, 5'- CGG GTC CTT CTT AGC ATC GT-3' and 5'-  
 AGA AGC AGC TTG CTT TTC TGA- 3'; hCCR5vB, 5'-ATC TGG CAT AGT CTC ATC TGG C-3' and 5'-  
 TAA TCC ATC TTG TTC CAC CCG-3'; hCCR7, 5'- ATG GAC CTG GGG AAA CCA AT- 3'and 5' - CGT



CCG TGA CCT CAT CTT GA - 3'; hIL6R, 5'- GTA CCA CTG CCC ACA TTC CT-3' and 5'-CCA CGT CTT CTT GAA CCT CAG-3'; hIL7R, 5'- GTC GTC TAT CGG GAA GGA GC-3' and 5'-TGG ATA AAT TCA CAT GCG TCC A-3'; hTGFB3, 5'- AAG TGG GCT TTG GAC AAT GG-3' and 5'-CAT CTC CCA TCT CCT CTG CAT T-3'; hFLT3, 5'- TCG AGG AGG GCA ACT ACT TT-3' and 5'-GGT GTC GTT TCT TGC CAC TG-3'; hCSF2RA, 5'-AGA CAG CAG ATC CGA GAA GC-3' and 5'- GAG AGA AGG GAA GAG CGA CA-3'; hKIT, 5'-GCA TTC AAG CAC AAT GGC AC- 3' and 5' - GGG ATG GAT TTG CTC TTT GTT G - 3'; hEGFR, 5'- TGC CAT CCA AAC TGC ACC TA - 3' and 5'- GGG ATC TTA GGC CCA TTC GT - 3'; hFGFR1, 5'- AAC CAA ACC GTA TGC CCG TA - 3' and 5'-AAC TTC ACT GTC TTG GCA GC - 3'; hIGF1R, 5'-CGT GGG AGG GTT GGT GAT TA - 3' and 5'- GAA CGT ACA CAT CAG CAG CG - 3'; hEPOR, 5'- TTC TGG TGT TCG CTG CCT A - 3' and 5'- GCG TCT AGG AGC ACT ACT TCA-3'; hTLR1, 5'-CAA GCA GGT TGT CTT GTG TTA AAG-3' and 5'-TCT TCT AAC GAG GAA GAG GGC-3'; hTLR2, 5'-GGT AGT TGT GGG TTG AAG CAC - 3' and 5' - GCC CTT GCA GAT ACC ATT GC - 3'; hTLR3, 5'-TCC CTT TGT CAA GCA GAA GAA TTT-3' and 5'- AGC TGA ACC TGA GTT CCT AAT TT-3'; hCXCR4, 5'-GCA GCA GGT AGC AAA GTG AC-3' and 5'- GAA GTG TAT ATA CTG ATC CCC TCC A-3'; hCSF2RB, 5'- CCC TCA ACG TGA CCA AGG AT - 3' and 5'- TCT CGG TCT TGC TGT CCT TC - 3'; hMYC, 5'- CTC CGT CCT CGG ATT CTC TG - 3' and 5'- TTC TTG TTC CTC CTC AGA GTC G - 3'; hOSM, 5'- GCT GCT CAG TCT GGT CCT T - 3' and 5'- TGT CTG CTT CTG GAG CTG G - 3'; hPIM1, 5'-CTT CGG CTC GGT CTA CTC AG-3' and 5'-TGC CAT TAG GCA GCT CTC C-3'; hFOS, 5'-GGA GAA TCC GAA GGG AAA GGA-3' and 5'-CTG TCT CCG CTT GGA GTG TA-3'; hRAF1, 5'-TGG CTC CCT CAG GTT TAA GAA-3' and 5'-GAT CGT CTT CCA AGC TCC CT-3'; hBCL2, 5'-ATG TGT GTG GAG AGC GTC AA-3' and 5'-GTT CCA CAA AGG CAT CCC AG-3'; hBCL2L1, 5'- CCT CTC CCG ACC TGT GAT AC-3' and 5'-TCT GAA GGG AGA GAA AGA GAT TCA A-3'; hJUN, 5'-TTT CTG GCC TGC CTT CGT TA-3' and 5'-ACA ACA CTG GGC AGG ATA CC-3'; hIL8, 5'- AGG AAG AAA CCA CCG GAA GG-3' and 5'-AAA CTG CAC CTT CAC ACA GAG-3'; hGCSF, 5'- CCA GAG CTT CCT GCT CAA GT-3' and 5'- TAG GTG GCA CAC TCA

CTC AC-3'; hHLA-DRA, 5'-TGG AGT CCC TGT GCT AGG AT-3' and 5'-TGT TCT TCT TTG ATA GCC CAT GA-3'; hCD34, 5'- TCT TGG GCA TCA CTG GCT ATT-3' and 5'-ATA AGG GTC TTC GCC CAG C-3'; hCD73, 5'- TGA TGA ACG CAA CAA TGG AAT C-3' and 5'- AGG GTC ATA ACT GGG CAC TC-3'; hCD90, 5'- TTC ACT AGC AAG GAC GAG GG-3' and 5'-ACC AGT TTG TCT CTG AGC ACT-3'; hCD105, 5'- CCT CAA CAT GGA CAG CCT CT-3' and 5'-CAC TCT GAC CTG CAC AAA GC-3'; hCD31, 5'- CCC ACA ACA GAC ATG GCA AC-3' and 5'-CTG CTG ACC TTG GAT ATG CG-3'; hDLL4, 5'-TGT CAT TGC CAC GGA GGT AT-3' and 5'-ATT CCC TCC TCC TCC TGA GA-3'; hIL21, 5'-ACA CAG ACT AAC ATG CCC TTC A-3' and 5'-AGA AGC AAA TCT GGA TAG GTA AAG A-3'; hIL15, 5'-TCC ATC CAG TGC TAC TTG TGT-3' and 5'-TGG GTA TAT TAG CTG CAT CCC AA-3'; hINS, 5'-AGG CCA TCA AGC AGA TCA CT-3' and 5'-GGT GTT GGT TCA CAA AGG CT-3'; hGAD67, 5'- GTT CGC ACA GGT CAT CCT C-3' and 5'-AGG ACA AAC ACT GGT GCA AT-3'; hPTPRN, 5'- TGC CCA CGG CTG TCT ATT T-3' and 5'-ACA CCT TGT AAG CGT TGG AGA-3'; hPLP1, 5'- AGA GGA CAA AGA TAC TCA GAG AGA A-3' and 5'-AAC AAG CCC ATG TCT TTG GG-3'; hATP4A, 5'- CCC AGA GTA CGT CAA GTT CG-3' and 5'-5'- GCG ATT GCC AGG TAC AGA TTG-3'; hCHRNA1, 5'- AAT GTG CGT CTG AAA CAG GG-3' and 5'- GTT GTA ATC CAC CCA TTG CTC A-3'; hTYRP2, 5'- CTT CCT GAA CGG GAC AAA CG-3' and 5'-TCA GTA AAG GAA TGA AGA ACC ACA-3'; hAFP, 5'- GAG GGA GCG GCT GAC ATT AT-3' and 5'-GCC AAC ACC AGG GTT TAC TG-3'; hSAG 5'-AGC TCC GTG CGA TTA CTG AT-3' and 5'-TTG AGA GAG ACC GCA AGG TG-3'; hATP4B, 5'- ACT ACG TGG CCT TCT ACG TG-3' and 5'-GTC TTG GTA GTC CGG TGT GT-3'; hALB, 5'- CGC CTT TGG CAC AAT GAA GT-3' and 5'- GCA TCT CGA CGA AAC ACA CC-3'.

### **Primary Culture of Unique Human Populations**

Generation of adipose derived stem cells (ADSCs) from the CD34+ HLA-DR- population isolated from human patient 2 was conducted using IMDM media supplemented with  $2 \times 10^{-3}$  M Hydrocortisone,  $2 \times 10^{-2}$  m 2-Mercaptoethanol, 10 ng/mL EGF. Adherent cells were isolated and

given the supplemented IMDM media in order to preferentially select ADSCs for growth [81]. To determine if the ADSCs were multipotent, differentiation of the cell line into chondrocytes myoblasts was conducted according to the protocols of Zuk et al 2002 [82]. For culturing of human CD34+ HLA-DR+ populations RPMI and DMEM with concentrations of 5-20% FBS were unsuccessfully used. Other unsuccessful growth attempts included using 3T3s irradiated at 4000 rads and using ADSCs derived from patient 2 as feeder cells.

## **Results**

### **HLA-DR, CD34 populations**

Isolation of lymph nodes from nine patients resulted in seven successful preparations of individual cells (Figure 21). Flow cytometric analysis focused on the CD45- stromal populations of the human lymph nodes and isolated the viable cells according to positive calcein violet presence. Two populations were clearly and repeatedly found in all seven patients: CD34+ HLA-DR+ and CD34- HLA-DR-, while two human subjects had a third population of CD34+ HLA-DR- cells. These two preparations involved retaining the surrounding fat around the lymph node follicle.

### **Flow cytometric profile of CD34+ HLA-DR+ cells.**

Relevant negative markers help define the CD34+ HLA-DR+ population (Figure22). CD19 is a B cell marker, further clarifying that our cell population is not a B cell. HLA-DQ is part of the heterodimer that is MHC-II complex in human cells. DLL-1 is Delta Like 1 and plays a role in Notch signaling pathway and hematopoiesis differentiation fate. It plays a major role in T cell development. CXCR5 is present in spleen and lymph node follicles and is a receptor for CXCL13 which helps control the organization of B cells within lymph node follicles. LYVE-1 and VEGFR3 negativity indicates that this cell population is not lymphatic endothelium [89, 90]. Also negative is CD106, VCAM cell adhesion molecule, which mediates adhesion of lymphocytes and monocytes to vascular endothelium. Gp38, podoplanin, is a marker of lymphatic endothelium and fibroblastic reticular cells (FRCs), but is absent from the isolated CD34+ HLA-DR+ cells.

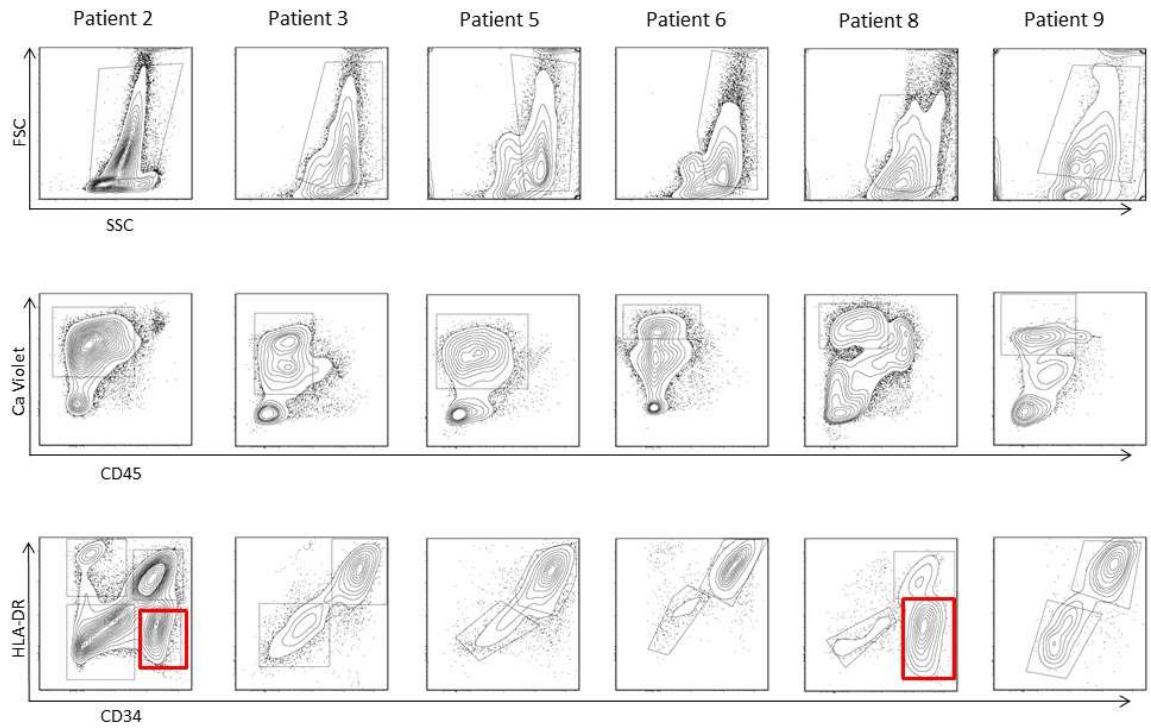


**Fig 21. Human lymph node digest and flow cytometric profile.** Nine healthy human patients underwent lymph node retrieval followed by lymph node digest and flow cytometric staining. Seven out of nine retrievals were successful while two resulted in poor yields and insufficient cell counts for analysis. Events were gates according to forward scatter and side scatter, followed by gating on the Ca Violet+ CD45- population—living, non-hematopoietic stromal cells. Finally CD34 and HLA-DR were used to identify two definitive populations: CD34+HLA-DR+ and CD34-HLA-DR-. In patients 2 and 8 more fat surrounding the lymph nodes was digested resulting in a third population of CD34+HLA-DR- cells.

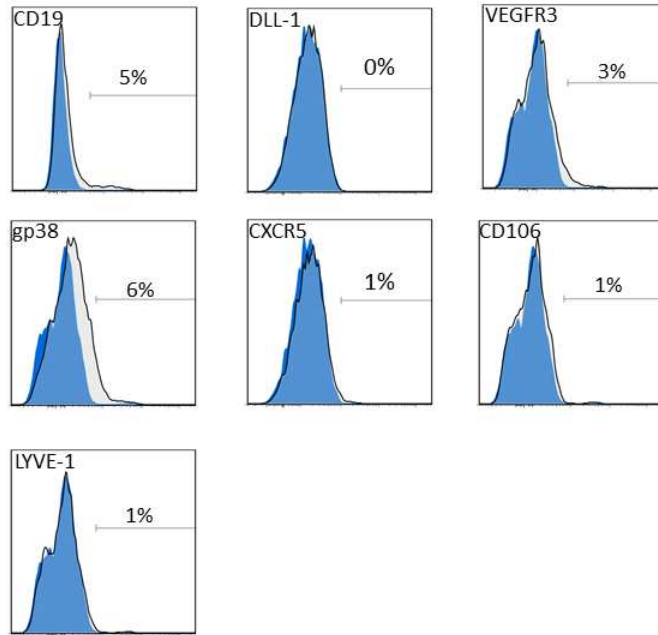


**Fig 22. Analysis of HLA-DR+ CD34+ surface profile (relevant negatives).** Isotypes corresponding to each constant region, species, and fluorophore were used for each analysis. Numbers indicate percent of mean fluorescent intensity (MFI) above the isotype control. Figures shown are representative of 2 independent patient sample analysis.

HLA-DR+ CD34+ cells isolated from the CD45- fraction of human lymph node tissue have high expression of SMA, HLA-ABC, CD31, CD73, CD90, CD105, CD144, and CD146 (Figure 23.  $\alpha$ -smooth muscle actin (SMA) is commonly found in smooth muscle cells and stains vessel walls [85]. HLA-ABC stains for human MHC-I present in all nucleated cells. Common markers for mesenchymal stem cells (MSCs) include CD73, CD90, CD105 [86]. CD144, also known as VE-Caderin, is responsible for cell adhesion and the permeability of endothelium [87]. CD146 is melanoma cell adhesion molecule responsible for cell cohesion and denotes endothelial cell lineage [88]. Lymphotoxin  $\beta$  Receptor (LTBR), CD123, and CD44 are strongly expressed on the surface of our isolated human population of cells. LtBR binds lymphotoxin  $\alpha$  and  $\beta$ , helps lymphatic vessels form, and is associated with apoptosis [35]. CD123 is the IL3 receptor and as such plays a role in signaling proliferation and growth. IL3 is released by activated T cells and can have many downstream effects when ligating the IL3 receptor [83]. CD44 is a glycoprotein hyaluronic acid receptor responsible for adhesion and migration [84].

**Gene expression profile of 3 populations: Adipose Derived Stem Cells (ADSCs), CD34+HLA-DR-, and CD34+HLA-DR+.**

Cells isolated from Patient 2 were analyzed for specific genes of interest related to growth factor receptors, cytokine signaling, chemokine trafficking, differentiation, presentation of antigen, co-stimulation, and stem-like indicators. Patient 2 cells were divided into freshly isolated CD34+ HLA-DR- and CD34+ HLA-DR+ populations. RNA was isolated from each population. ADSCs were derived from the CD34+ HLA-DR- population given specific media as outlined in materials and methods.

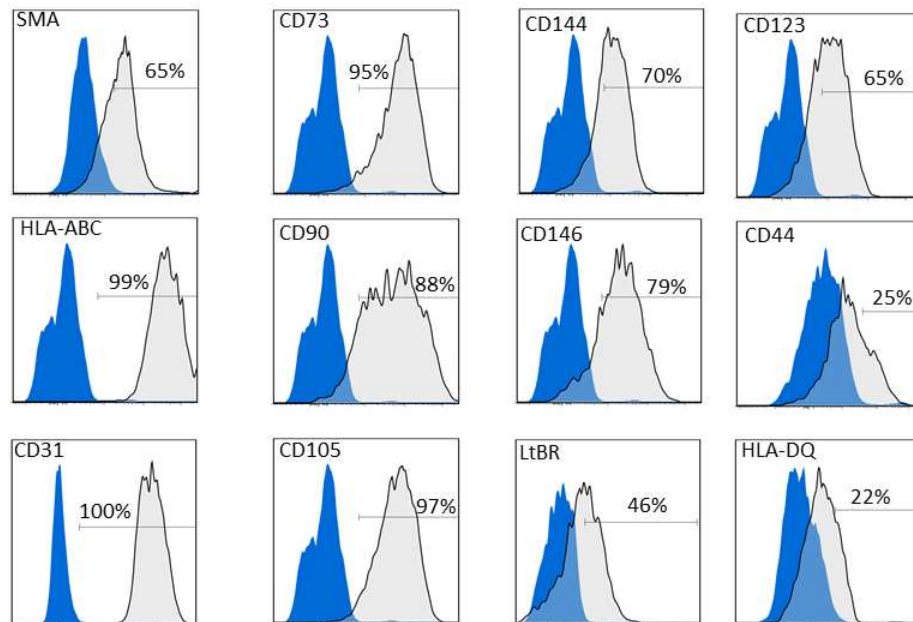


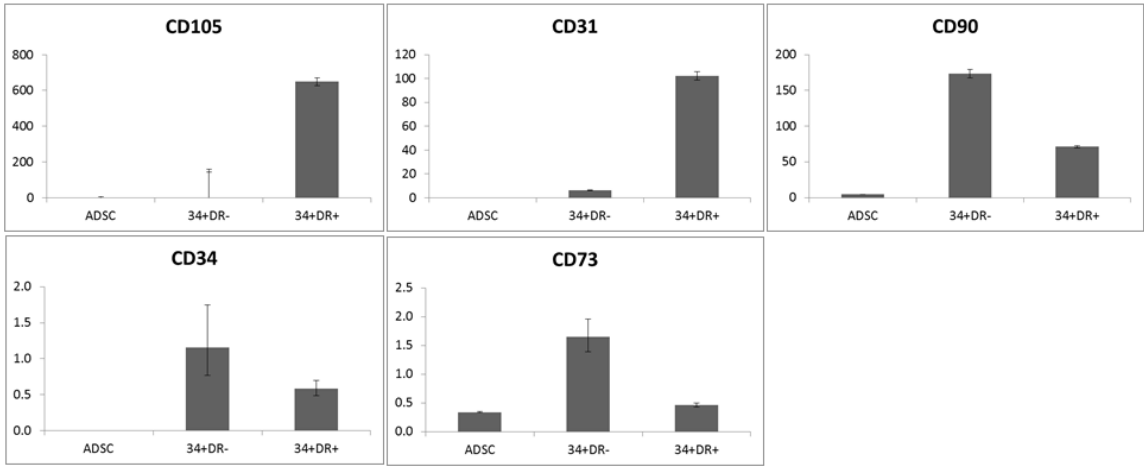
**Fig 23. Analysis of HLA-DR+ CD34+ flow cytometric profile (positive markers).** Isotypes corresponding to each constant region, species, and fluorophore were used for each analysis. Numbers indicate percent of mean fluorescent intensity (MFI) above the isotype control. Figures shown are representative of 2 independent patient sample analysis.



Focusing on the CD34+HLA-DR+ population, one sees that our flow cytometric profile corresponds to the gene expression profile in our positive flow controls (Figure 24). Growth factors expressed by our CD34+ HLA-DR+ cell population were also analyzed in order to elucidate possible autocrine growth mechanisms used by the cell (Figure 24). Analysis demonstrates high expression of VEGFC, a growth factor essential for maintaining and repairing vasculature.

Further qPCR analysis focused on receptors present on the surface of our double positive (CD34+ HLA-DR+) population (Figure 25). Receptor studies help shed light on possible signaling pathways and growth factors that may be essential for establishing a primary culture. The receptor for IL7R, EGFR, and TGFBR3 are all expressed in a relatively high amount, leading to a presumption that the corresponding ligands (IL-7, EGF, and TGF $\beta$ ) may play a role in our population's growth. TGFBR3 is a receptor for basic fibroblast growth factor (bFGF). IL3R was also found to have relatively high expression and was further analyzed by studying downstream molecules important in IL-3 signaling. Analysis of various cytokines and chemokines (Figure 26) demonstrates the high expression of IL-7 and IL-8. IL-7 is a hematopoietic growth factor produced by DCs and epithelial cells and is important in B and T cell development [91]. IL-8 is a neutrophil chemotactic factor and promotes angiogenesis [92]. The possible role of lymph node stromal cells in extra-thymic T cell development was analyzed with qPCR by studying genes involved in antigen processing and promiscuous antigen expression (Figure 27). HLA-DM is essential for loading antigen onto MHC-II for presentation to T cells. Promiscuous antigens, if expressed in the periphery can possibly eliminate self-reactive T cells. Finally, T cell development and IL3RA signaling molecules were analyzed via qPCR (Figure 28).

Positive Flow Cytometry Controls



Growth Factors

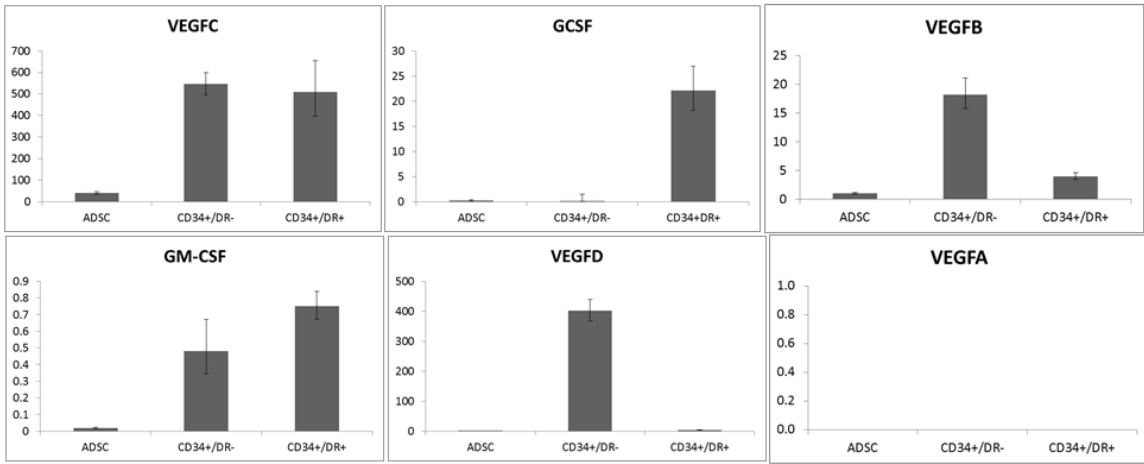


**Fig 24. qRT-PCR (Panel 1 – Positive Flow Controls and Growth Factors) - Relative expression (%Gapdh) of genes using in 3 populations: Adipose Derived Stem Cells (ADSCs), CD34+HLA-DR- and CD34+HLA-DR+. All samples were derived from patient 2 and linearly amplified. Results shown are taken from one patient sample analyzed in triplicate.**

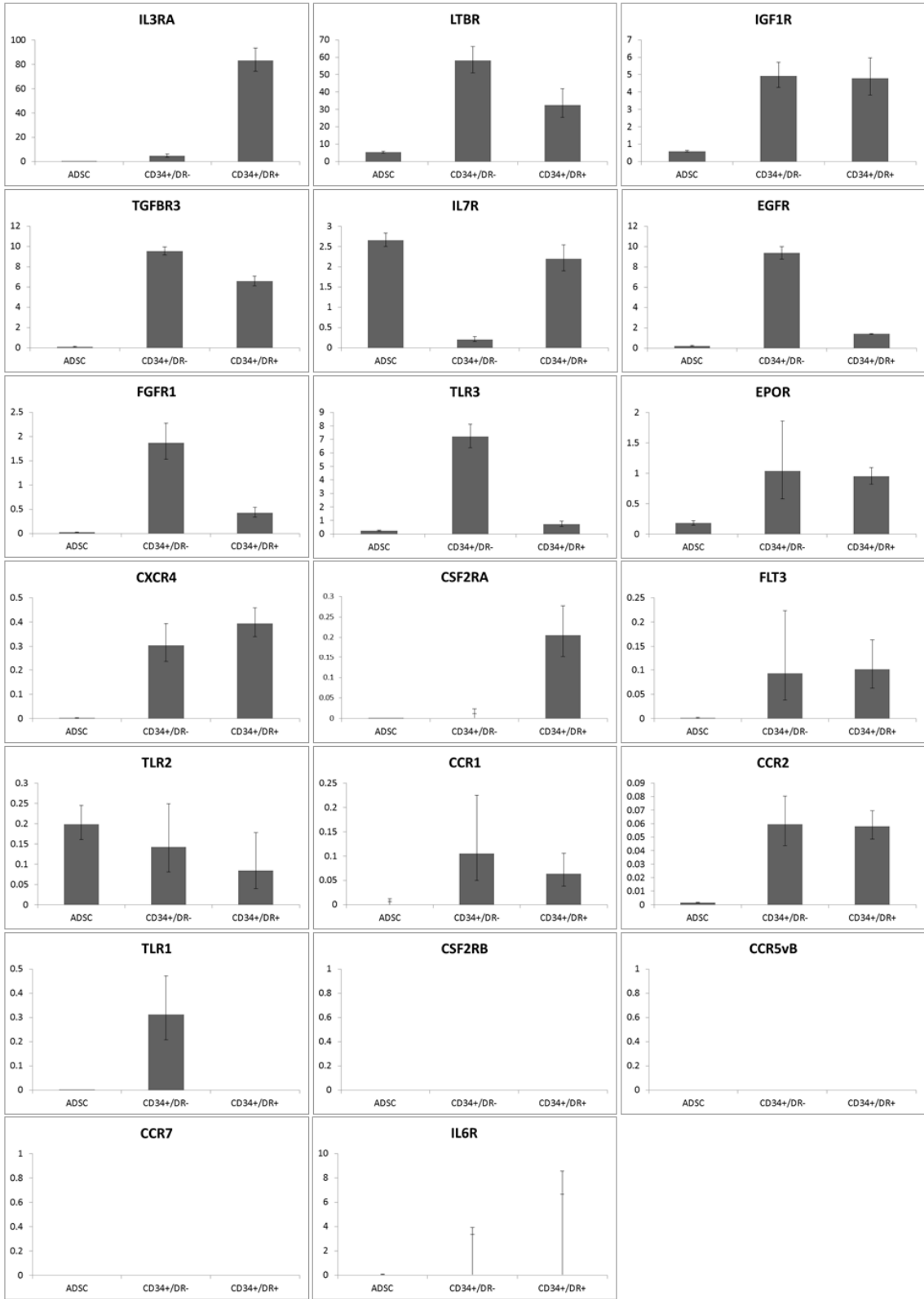


**Fig 25. qRT-PCR (Panel 2 – Surface Receptors)**

**Fig 25. qRT-PCR (Panel 2 – Surface Receptors)** Relative expression (%Gapdh) of genes using in 3 populations: Adipose Derived Stem Cells (ADSCs), CD34+HLA-DR and CD34+HLA-DR+. Growth factor, cytokine, and chemokine receptors were analyzed for expression between 3 populations of cells. Results shown are taken from one patient sample analyzed in triplicate.

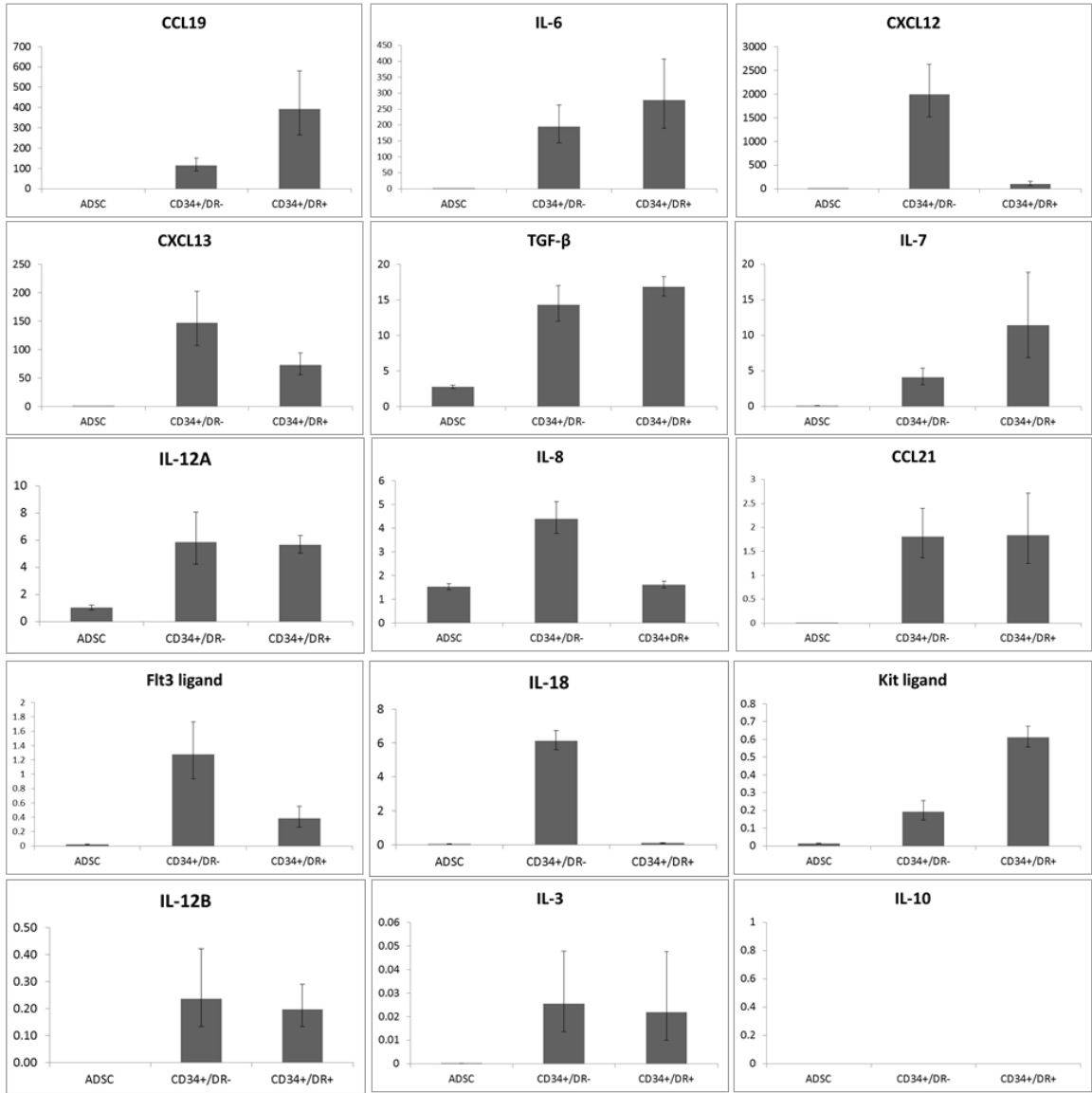


**Fig 26. qRT-PCR (Panel 3 – Cytokines and Chemokines).**

**Fig 26. qRT-PCR (Panel 3 – Cytokines and Chemokines).** Relative expression (%Gapdh) of genes using in 3 populations: Adipose Derived Stem Cells (ADSCs), CD34+HLA-DR and CD34+HLA-DR+. Analysis of various cytokine and chemokine production gene expression elucidated more functional properties of our CD34+HLA-DR+ population of interest. Results shown are taken from one patient sample analyzed in triplicate.

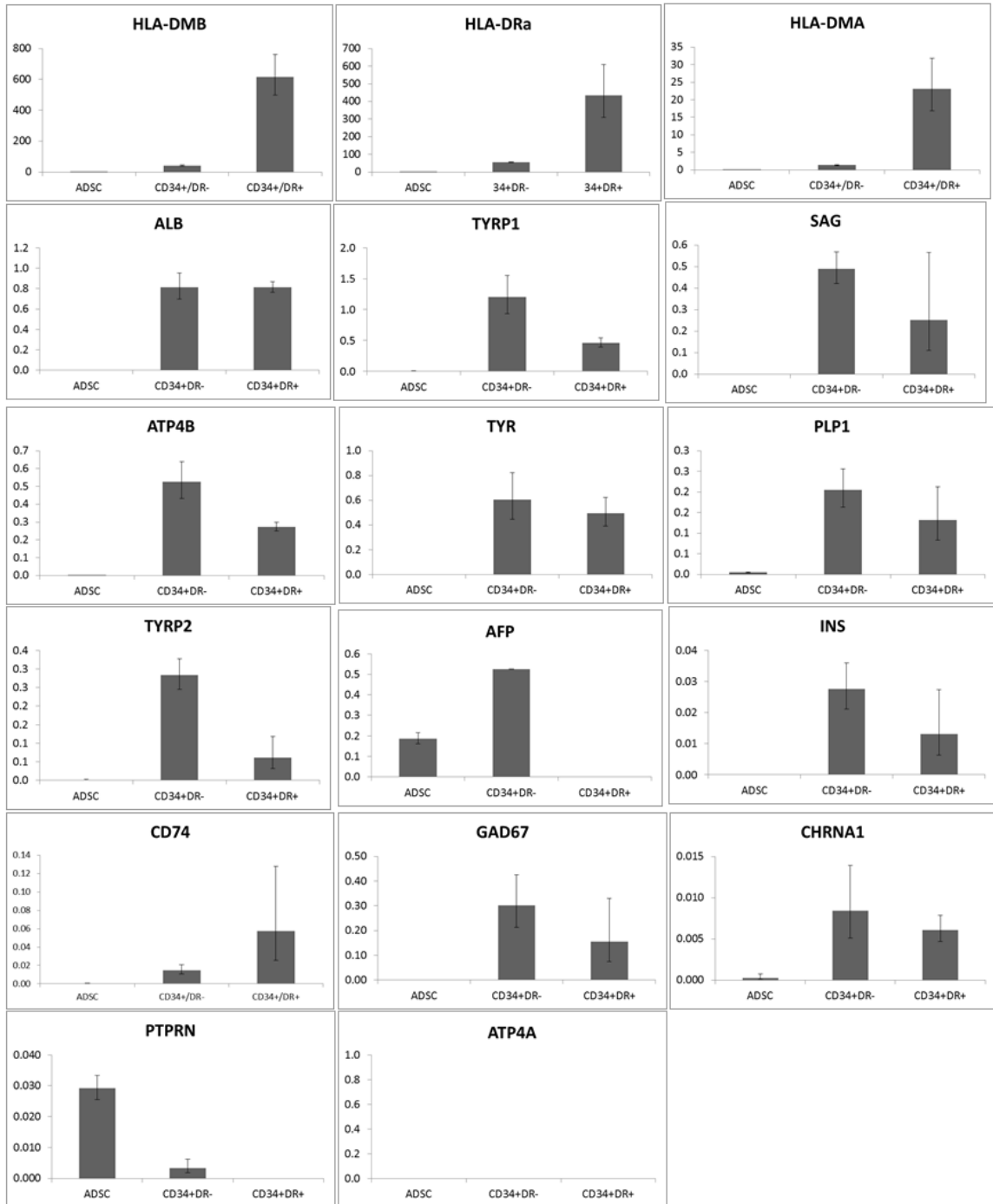
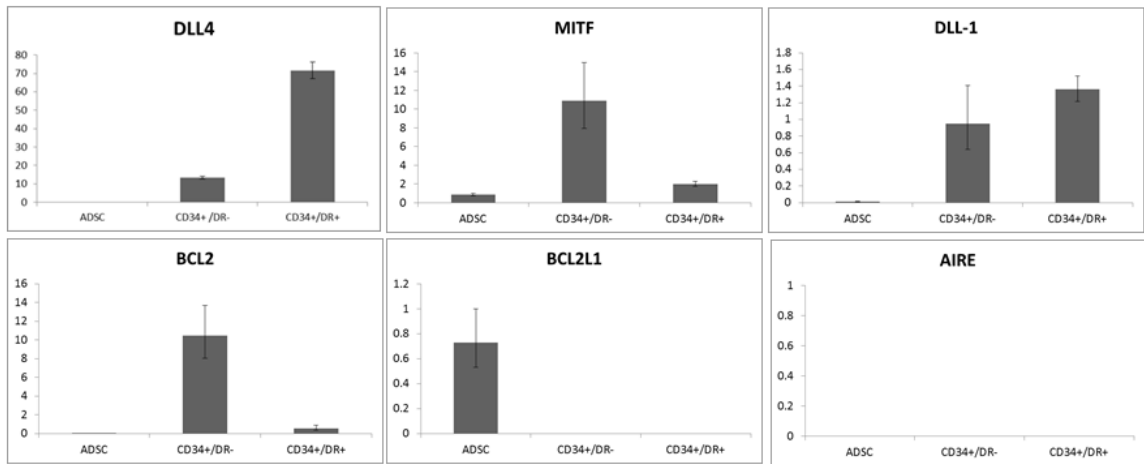


**Fig 27. qRT-PCR (Panel 4 – Antigen Processing and Promiscuous Self-Antigens).**

**Fig 27. qRT-PCR (Panel 4 – Antigen Processing and Promiscuous Self-Antigens).** Relative expression (%Gapdh) of genes using in 3 populations: Adipose Derived Stem Cells (ADSCs), CD34+HLA-DR and CD34+HLA-DR+. Promiscuous self-antigens involved in extra-thymic T cell education were also analyzed in our populations of interest. Results shown are taken from one patient sample analyzed in triplicate.



## T cell development



## IL3R Downstream Signaling

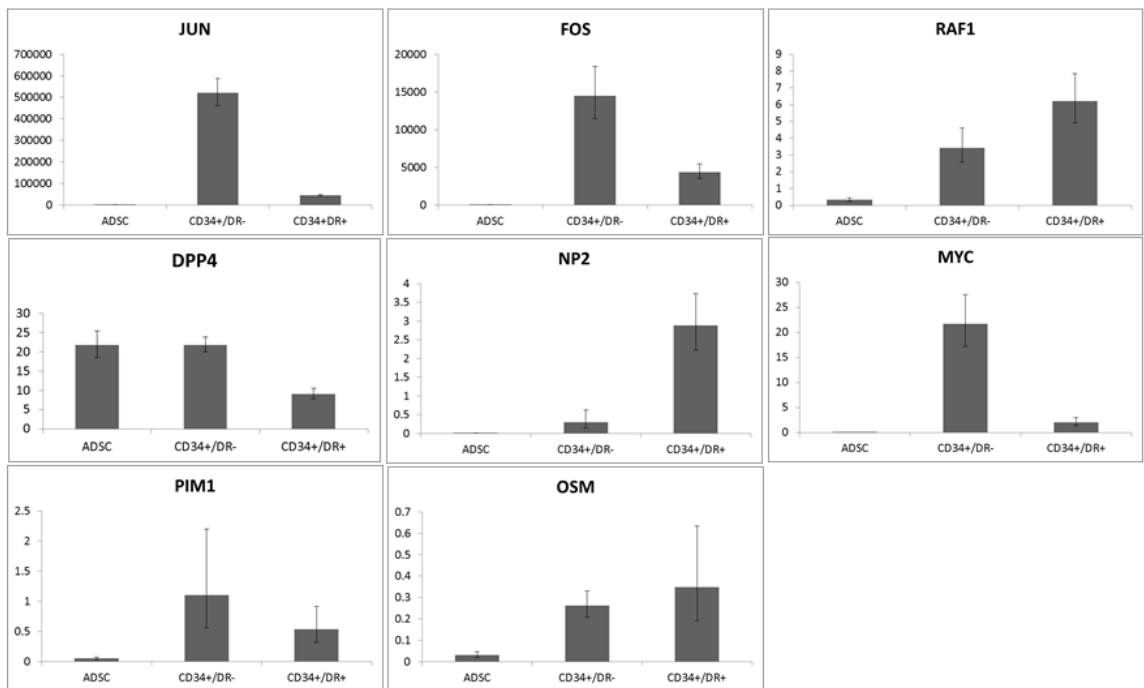


**Fig 28. qRT-PCR (Panel 5 – T Cell Development and IL3R Downstream Signaling).**

**Fig 28. qRT-PCR (Panel 5 – T Cell Development and IL3R Downstream Signaling).** Relative expression (%Gapdh) of genes using in 3 populations: Adipose Derived Stem Cells (ADSCs), CD34+HLA-DR and CD34+HLA-DR+. Analysis of molecules involved in thymic T cell development including AIRE – the driving force behind promiscuous self-antigen presentation. IL3R signaling was analyzed due to the high levels of IL3R RNA expression analyzed previously. Results shown are taken from one patient sample analyzed in triplicate.

AIRE is the driving force behind expression of promiscuous antigen in the thymus, but was not present in our lymph node stromal populations. DLL1 and DLL4 are important to T cell development and maturation [93]. Zúñiga-Pflücker's lab has successfully differentiated multipotent hematopoietic stem cells into T cells using DLL1 and DLL4 expressed by OP9 cells.

### **Histology of human lymph nodes**

Histology of a lymph node with its surrounding tissue revealed the presence of CD34 and HLA-DR in channels surrounding the lymph node (Figure 29). The HLA-DR+ CD34+ stains could not be assessed together due to lack of sufficient antibody staining, but individual stains using one of the two markers were used along with the endothelial marker SMA. The channels formed demonstrate a polarity of cells. Smooth muscle actin positivity is present on the exterior of the channel while the interior lumen is CD34+. HLA-DR positivity is located directly in the lumen of the peri-lymph node channels.

### **Growth attempts of CD34+ HLA-DR+ lymph node cells**

In order to further study the CD34+ HLA-DR+ cells we decided to initiate primary cultures. This would allow us to accomplish several things: 1) Identify the similarities between freshly isolated and cultured CD34+ HLA-DR+ cells. 2) Generate a cell line to provide unlimited cells for analysis and experimental study 3) Utilize large quantities of grown EpCAM+ cells for co-culture experiments with T cells.

The most successful growth attempt included plating CD34+ HLA-DR+ cells directly onto ADSCs derived from patient 2 tissue (Figure 30). Analysis of the primary culture identified a small population of HLA-DR+ cells with a small proportion of these being CD31+ (Figure 31).

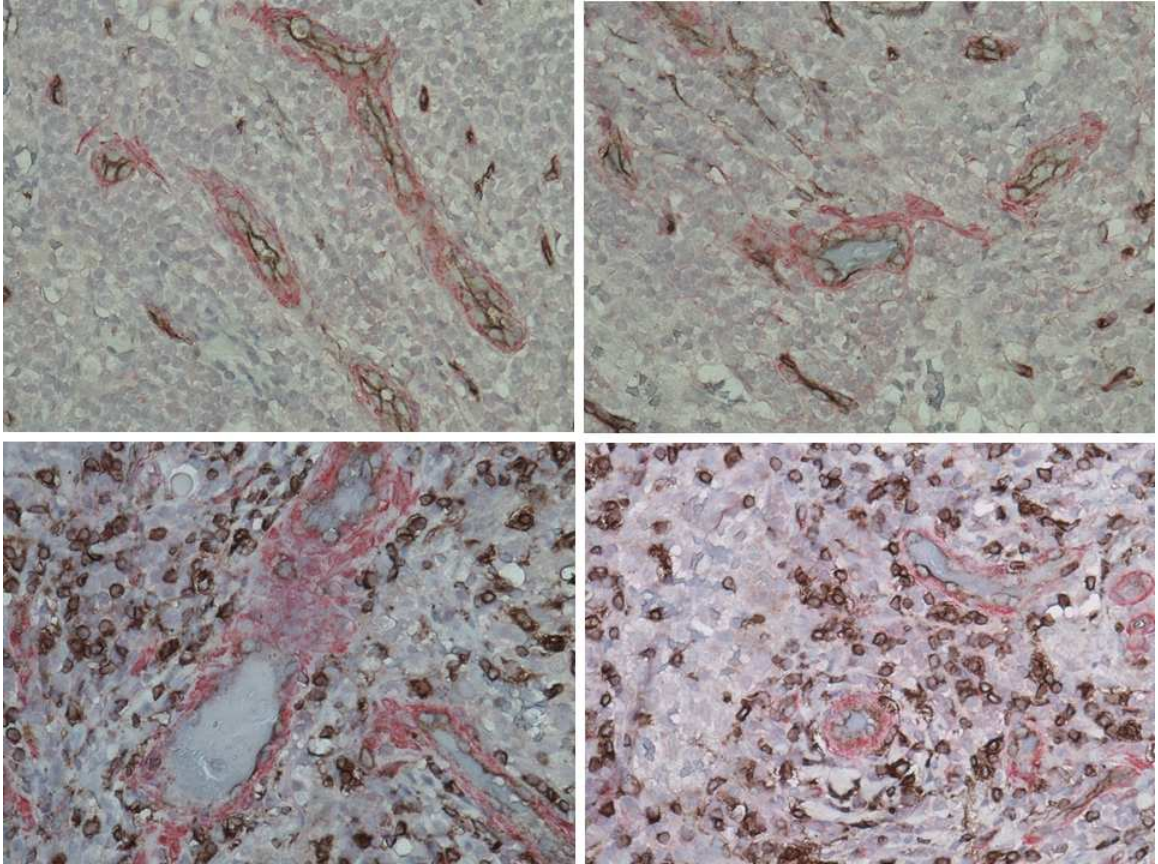


**Fig 29. Patient 2 lymph node and surrounding tissue histology.** Analysis of paraffin embed blocks of human lymph node cut to 5um thickness. **Top Panels:**  $\alpha$ -SMA-Red, CD34-Brown. **Bottom Panels:**  $\alpha$ -SMA-Red, HLA-DR-Brown.

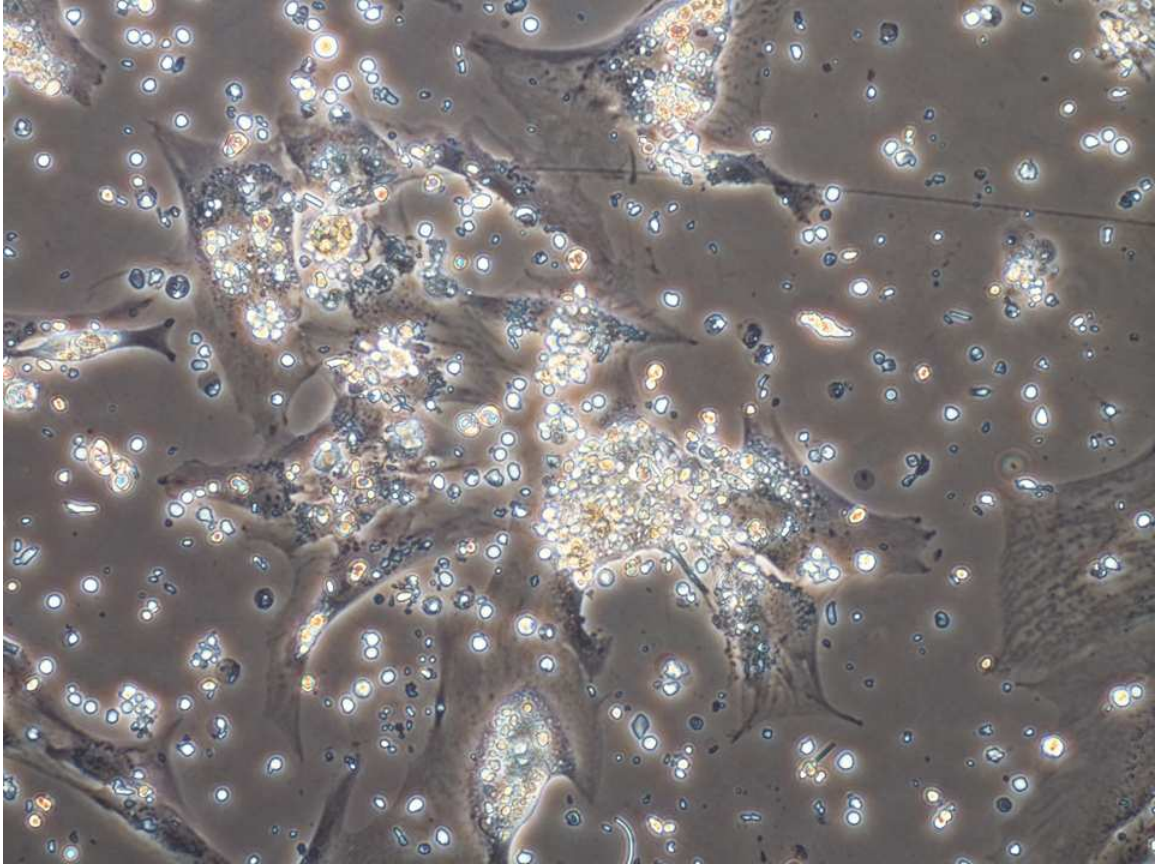


**Fig 30. Growth attempts of human CD34+ HLA-DR+ lymph node cells.** Patient 8 HLA-DR+ cells were isolated and placed directly onto ADSCs for support.

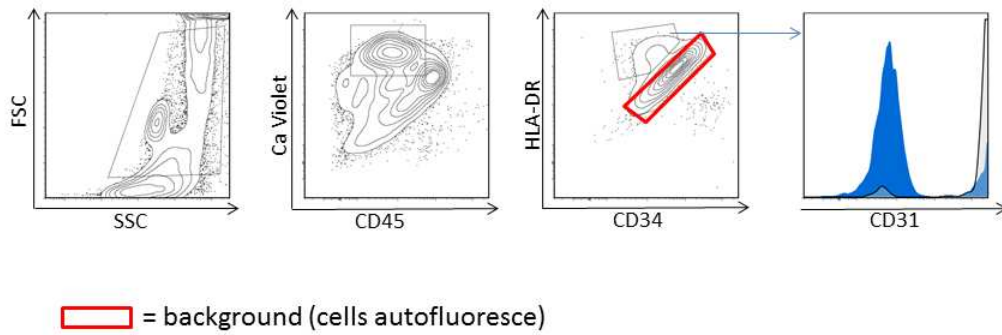


**Fig 31. Growth attempts of human CD34+ HLA-DR+ lymph node cells (Flow Cytometry).** Flow cytometric analysis of the grown population indicated that there is a small population of HLA-DR+ cells that with a small proportion of these also being CD31 positive.

## DISCUSSION AND FUTURE DIRECTIONS

### **Chapter 1. Lymph Node Stroma of the Mouse**

The two cell populations isolated in the lymph node stroma of mice play an important role in modulating the immune response. Ly51+ cells, capable of up-taking exogenous antigen, can stimulate CD4 and CD8 T cells to elicit a positive immune response, while EpCAM+ cells can inhibit T cell activation and proliferation through an unknown mechanism. These two cells may act in a complex system of checks and balances to ensure the proper immune response is spurred. The importance of the Ly51+ cells lies in its ability to present antigen and activate T cells. The escalating immune response needs a counter balance to control inflammation and proliferation of T cells. We believe the EpCAM+ cell population may be responsible for regulating hyper-stimulation of T cells and inflammation. The immune response must be appropriate for the stimulation. Foreign malicious bacteria or viruses must be dealt with efficiently while still maintaining control of inflammation and cell-mediated killing. Auto-reactive T cells must be eliminated or inhibited before causing damage to native cells. We believe the EpCAM+ and Ly51+ cells, located in and around the skin-draining lymph nodes, play a major role in balancing the immune response.

The Ly51+ cell population isolated from skin-draining lymph nodes of mice represents a novel stimulatory mechanism of T cells. The importance of this cell type will be analyzed by others in the laboratory, while my focus is on the more inhibitory function of the EpCAM+ cell population.

Evidence from histology, qPCR, and flow cytometry indicate that EpCAM+ cells may reside in the luminal surface of afferent or efferent lymphatic vessels surrounding the lymph node. This luminal layer of EpCAM+ cells is then surrounding by an SMA+ cell layer. These cells may inhibit

stimulated T cells when exiting the lymph node, regulating the immune response and controlling inflammation. The importance of adhesion molecules present on EpCAM+ cells may help leukocyte rolling and interaction and could also play a role in slowing the T cells down to enable EpCAM+ cells to have direct contact-mediated inhibition through an as yet un-described mechanism.

Results from initial phenotypic analysis of our two mouse populations, Ly51+ and EpCAM+, demonstrates the respective endothelial and epithelial nature of our population. The characteristic endothelial markers CD31, CD34, LYVE-1, and  $\alpha$ -SMA are present on our Ly51+ population, while the EpCAM+ population expresses the epithelial markers EpCAM and PCK. The EpCAM+ population can be divided into two further sub populations, gp38+ and gp38-. The functional difference between these two populations has not been elicited, but it may indicate a relation to the gp38+ and gp38- populations of stromal cells previously characterized in the lymph node follicle itself (FRCs and FDCs) [47]. The difference between these classical characterizations of stroma and our populations lies in the peri-nodal location of our EpCAM+ population while the classical conventions show gp38+ and gp38- populations inside of the node. This may indicate that the EpCAM+ cells are integral to lymphatic vessels that extend into the follicle itself, but with dissipating expression of EpCAM on intra-nodal lymphatic vessels.

EpCAM+ cells express a variety of surface proteins that could play a functional role in T cell trafficking, signaling, adhesion, and multipotency. The presence of adhesion molecules such as CD54 could play a role in adhering to passing leukocytes, bringing them into proximity to the inhibitory mechanisms of EpCAM+ cells. Surface markers such as PDL1, LtBR can play a role in cell signaling, and possibly enable the EpCAM+ cells to directly inhibit T cells. EpCAM+ cells



express a variety of stem-like markers (CD38, CD44, CD140a, CXCR4, OCT4, Sca-1, CD9, and CD29) which indicate the multi-potent potential of the EpCAM+ cells. These cells may act in a progenitor fashion or have a high proliferative capacity to restore epithelial lining of damaged lymphatic vessels.

EpCAM+ cells could be inhibiting activated T cells through a variety of mechanisms. They are capable of inhibiting both artificially bead-activated T cells and T cells activated by antigen presenting dendritic cells with specific antigen. The cells are capable of inhibition through both a secretory system (transwell model) or through direct contact (U-bottom), but have the most dramatic inhibition when direct contact is present. The loss of IL-2 production by T cells inhibited by EpCAM+ cells can lower the proliferative capacity of T cells. The ability of EpCAM+ cells to retain activated T cells in their naïve CD44-CD62L+ state also demonstrates the suppressive force of EpCAM+ cells.

We have developed a possible model for how EpCAM+ cells are inhibiting T cells (Figure 32). When T cells are activated by an APC presenting specific antigen in the context of MHC I or MHC II, along with co-stimulation, IFN $\gamma$  and TNF $\alpha$  are produced. EpCAM+ expressing IFN $\gamma$  and TNF $\alpha$  receptors may induce a signaling cascade resulting in JAK1+2 phosphorylating STAT1, causing translocation of STAT1 into the nucleus, causing up-regulation of the iNOS and IDO1 genes. IDO1, when activated, converts tryptophan into kynurenine, depleting essential tryptophan that is necessary for T cell growth and proliferation. Kynurenine may also play a role in apoptosis of T cells through signaling pathways of the T cell [40]. iNOS up-regulation leads to the production of Nitric Oxide, a potent to combine with superoxides to form peroxynitrites; a

free radical capable of damaging DNA, lipids, and proteins [44]. PDL1 and LtBR may cause contact-mediated inhibition or induce apoptosis of the activated T cell.

The isolated cell populations serve as a model for further studies of human lymph node and peri-lymph node stromal populations. If similar cell types are identified in humans, they could be important to autoimmune diseases or even immunosuppressed patients. The exact mechanism of EpCAM+ inhibition of T cells could have clinical significance in patients undergoing bone marrow transplants, helping T cell recovery following irradiation and transplantation.

### **Future Studies**

Successful growth studies will be continued to analyze the effect of feeder populations, such as LA7 and 3T3 fibroblasts, and their effect on the growth and maintenance of an EpCAM+ primary culture. The successful growth of EpCAM+ cells using confluent LA7 cells as feeders indicates that 3T3 fibroblast may also be used at higher concentrations to elicit similar growth. Previous studies using 3T3s used lower concentrations of 3T3's and resulted in unsuccessful growth of EpCAM+ cells. Another culturing goal is to successfully and repeatedly grow gp38+ EpCAM+ cells. We believe that our current isolation method using column selection removes the EpCAM<sup>low</sup> population which is the same population that has the gp38 positivity. By only depleting CD45+ cells we may be able to successfully grow both EpCAM+ gp38- and EpCAM<sup>low</sup> gp38+ cell populations. Further analysis will be conducted to elicit the functional difference between these two populations.

To elicit the actual mechanism of EpCAM+ cell inhibition of activated T cells a number of studies are necessary. Currently the only evidence of specific mechanisms is resultant from qPCR and

flow cytometry data. It will be necessary to measure directly the levels of nitric oxide resultant from iNOS up-regulation and kynurenine and tryptophan levels due to up-regulation of IDO1. Further studies will be required to determine if one or more mechanisms is responsible. These include blocking the release of IFN $\gamma$  (IFN $\gamma$  knockout T cells) and blocking IFN $\gamma$  and IFN $\gamma$ R by using specific antibodies ( $\alpha$ -IFN $\gamma$  and  $\alpha$ -IFN $\gamma$ R). We would also like to block the TNF $\alpha$  and TNF $\alpha$ R signaling using specific antibodies ( $\alpha$ -TNF $\alpha$  and  $\alpha$ -TNF $\alpha$ R). Further studies will need to employ the use of IDO1 and iNOS knockout mice to isolate EpCAM+ cells and determine if these knockout cells are still able to functionally inhibit activated T cells. The use of chemical inhibitors of IDO1 and iNOS such as 1-methyl-tryptophan (1-MT) and Aminoguanidine hydrochloride (AG) will also be helpful in eliciting the exact mechanism of EpCAM+ cell inhibition of T cells. Further experiments will also require the blocking of surface markers PDL1 and LtBR which could be responsible for direct contact inhibition. This will be accomplished by using specific blocking antibodies ( $\alpha$ -PD-L1 and  $\alpha$ -LtBR).

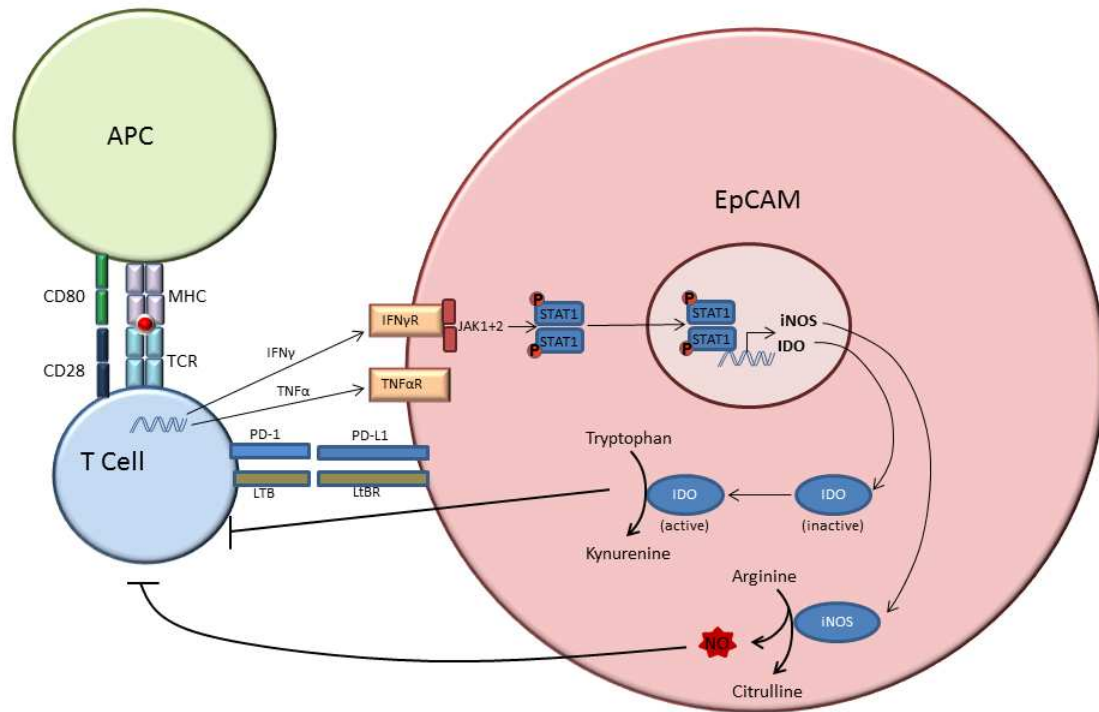


**Fig 32. Proposed model of the inhibitory action of EpCAM+ cells on activated T cells.** Antigen presenting cells present antigen to a specific TCR with costimulation, activating the T cell and causing proliferation and production of the cytokines IFN $\gamma$  and TNF $\alpha$ . EpCAM+ cells, when encountering IFN $\gamma$  and TNF $\alpha$  may upregulate iNOS and IDO resulting in depletion of essential tryptophan and production of the nitric oxide. This leads to T cell inhibition or killing. Future studies will involve blocking each step in this process to elicit the exact mechanism of T cell inhibition by EpCAM+ cells.

## **Chapter 2. Human Lymph Node Stroma.**

The human lymph node studies efficiently characterized the lymph node stroma present in skin-draining lymph nodes of healthy donors. The CD34+ HLA-DR+ population of interest isolated from lymph nodes appears to be analogous to the Ly51+ MHCII+ population isolated from mouse lymph nodes. While no functional co-cultures of human lymph node stroma were conducted, the potential for a stromal cell of lymph node origin to stimulate T cells is important. The human CD34+ HLA-DR+ population and the Ly51+ MHCII+ population have similar expression of endothelial markers CD31, CD34, and of course MHCII+.

The CD34+ HLA-DR+ population expresses multiple markers for mesenchymal stem cells (MSCs) including the canonical CD73, CD90, and CD105. The importance of this stem-like phenotype lies in the potential for this cell to differentiate and repopulate damaged lymph nodes, possibly capable of generating adipose or vasculature necessary for lymph node repair.

The high expression of DLL-4 in the CD34+ HLA-DR+ population could have major implications in the study of extra-thymic T cell development. [93]. Zúñiga-Pflücker's lab has successfully differentiated HSCs into T cells using OP9 cells that express DLL-4. Our isolated cell population could be responsible for development of T cells outside of the thymic environment. The mouse Ly51+ population is analogous in many ways, including the expression of DLL4. If these cell populations are capable of innately differentiating HSCs into T cells, it will be a breakthrough in T cell development studies.

One important gene expression assay concluded that IL3R was upregulated in the CD34+ HLA-DR+ population. IL-3R is a transmembrane molecule that initiates signaling through recruitment

of the  $\beta$  chain of the receptor followed by the Janus kinase and STAT pathway, the mitogen-activated protein kinase pathway and the phosphatidylinositol 3-kinase pathway. These pathways can lead to cell proliferation and prevention of apoptosis. IL-3 stimulation also is integral to differentiation of multipotent hematopoietic cells into basophils and mast cells. While our cell is of non-hematopoietic origin, the IL-3 signaling may still play a role in differentiation of tissue [94]. To further analyze the IL-3R pathway, signaling molecules within the pathway were studied including MYC, OSM, PIM1, FOS, RAF1, BCL2, and JUN.

Histology of the human lymph nodes and the surrounding tissue shows the anatomical relevance of our cell population. CD34 and HLA-DR are present on the luminal face of channels in the adipose tissue surrounding the lymph node. These cell types are surrounded by SMA+ cells. The polarity of HLA-DR+ expression on the interior of channels may play an important role in stimulating T cells migrating through these channels.

### **Future Studies**

Many studies need to be further analyzed in considering the functional role of the CD34+ HLA-DR+ cell population present in human lymph nodes. Based on the analysis of possibly analogous mouse stroma, the human lymph node stroma could be capable of up-taking exogenous antigen and presenting and stimulating migrating T cells. Studies isolating the population of interest and analyzing the capability of the cell to up-take and present antigen need to be pursued. If the cell is capable of uptaking antigen and presenting in context of MHCII, the CD34+ HLA-DR+ cells need to be studied for their capability of stimulating T cells in an in-vitro setting.

The difficulty in these studies is the minimal number of cells recovered from a preparation of human lymph node tissue. To attain the necessary cell numbers to analyze the functional role of human lymph node stroma, one must first successfully culture the CD34+ HLA-DR+ cells and analyze the cultured cell line for any discrepancies to the freshly isolated cells. Successful growth of CD34+ HLA-DR+ cells will enable a full analysis of functional properties. The analysis of growth factor receptors gives us clues into the optimal growth conditions for CD34+ HLA-DR+ cells.

T cell development studies will need to be conducted to analyze the role DLL-4 is playing in differentiating HSCs into T cells extra-thymically. Isolated CD34+ HLA-DR+ cells will be cocultured with isolated human HSCs or T cell progenitors and analyzed for differentiation into T cells.

Another important goal is to identify an epithelial cell population analogous to the EpCAM+ population in mice. The isolation of a population of human lymph node stromal cells capable of inhibiting T cell activation and proliferation will be a major breakthrough in the study of immunology. It will be necessary to analyze multiple markers of epithelial.

The presence of multi-potent markers such as CD73, CD90, and CD105 indicates the possible role of this CD34+ HLA-DR+ population in differentiation and proliferation. By using different growth factors and cytokines, we can analyze the differentiation capacity of the CD34+ HLA-DR+ population. Because of the similarities between our isolated population and MSCs, we will need to analyze the ability of our population to differentiate into cells of adipogenic, osteogenic, chondrogenic, and myogenic lineages.

## REFERENCES

1. Itano, A.A. and M.K. Jenkins, *Antigen presentation to naive CD4 T cells in the lymph node*. Nature immunology, 2003. **4**(8): p. 733-739.
2. Katakai, T., et al., *Lymph node fibroblastic reticular cells construct the stromal reticulum via contact with lymphocytes*. The Journal of experimental medicine, 2004. **200**(6): p. 783-795.
3. Lee, J.-W., et al., *Peripheral antigen display by lymph node stroma promotes T cell tolerance to intestinal self*. Nature immunology, 2006. **8**(2): p. 181-190.
4. Derbinski, J., et al., *Promiscuous gene expression in medullary thymic epithelial cells mirrors the peripheral self*. Nat Immunol, 2001. **2**(11): p. 1032-1039.
5. Schwarz, B.A. and A. Bhandoola, *Trafficking from the bone marrow to the thymus: a prerequisite for thymopoiesis*. Immunological Reviews, 2006. **209**(1): p. 47-57.
6. Allman, D., et al., *Thymopoiesis independent of common lymphoid progenitors*. Nat Immunol, 2003. **4**(2): p. 168-174.
7. Adolfsson, J., et al., *Upregulation of Flt3 Expression within the Bone Marrow Lin-Sca1+c-kit+ Stem Cell Compartment Is Accompanied by Loss of Self-Renewal Capacity*. Immunity, 2001. **15**(4): p. 659-669.
8. D'Amico, A. and L. Wu, *The Early Progenitors of Mouse Dendritic Cells and Plasmacytoid Predendritic Cells Are within the Bone Marrow Hemopoietic Precursors Expressing Flt3*. The Journal of Experimental Medicine, 2003. **198**(2): p. 293-303.
9. Germain, R.N., *T-cell development and the CD4-CD8 lineage decision*. Nature Reviews Immunology, 2002. **2**(5): p. 309-322.
10. Godfrey, D.I., et al., *A developmental pathway involving four phenotypically and functionally distinct subsets of CD3-CD4-CD8-triple-negative adult mouse thymocytes defined by CD44 and CD25 expression*. The Journal of Immunology, 1993. **150**(10): p. 4244-4252.
11. Bruno, L., et al., *Threshold of pre-T-cell-receptor surface expression is associated with alphabeta T-cell lineage commitment*. Curr Biol, 1999. **9**(11): p. 559-68.
12. Hozumi, K., et al., *Delta-like 4 is indispensable in thymic environment specific for T cell development*. The Journal of Experimental Medicine, 2008. **205**(11): p. 2507-2513.
13. Schmitt, T.M. and J.C. Zúñiga-Pflücker, *Induction of T cell development from hematopoietic progenitor cells by delta-like-1 in vitro*. Immunity, 2002. **17**(6): p. 749-756.
14. Kisielow, P., et al., *Positive selection of antigen-specific T cells in thymus by restricting MHC molecules*. Nature, 1988. **335**(6192): p. 730-733.
15. Gray, D.H., et al., *Unbiased analysis, enrichment and purification of thymic stromal cells*. Journal of immunological methods, 2008. **329**(1): p. 56-66.
16. Hernández-Hoyos, G., et al., *Lck activity controls CD4/CD8 T cell lineage commitment*. Immunity, 2000. **12**(3): p. 313-322.
17. Ueno, T., et al., *CCR7 signals are essential for cortex-medulla migration of developing thymocytes*. J Exp Med, 2004. **200**(4): p. 493-505.
18. Liston, A., et al., *Aire regulates negative selection of organ-specific T cells*. Nature immunology, 2003. **4**(4): p. 350-354.
19. Anderson, M.S., et al., *The Cellular Mechanism of Aire Control of T Cell Tolerance*. Immunity, 2005. **23**(2): p. 227-239.
20. Starr, T.K., S.C. Jameson, and K.A. Hogquist, *Positive and negative selection of T cells*. Annual review of immunology, 2003. **21**(1): p. 139-176.
21. Gray, D., et al., *Proliferative arrest and rapid turnover of thymic epithelial cells expressing Aire*. The Journal of experimental medicine, 2007. **204**(11): p. 2521-2528.



22. Lohse, A.W., et al., *Estimation of the Frequency of Self-reactive T cells in Health and Inflammatory Diseases by Limiting Dilution Analysis and Single Cell Cloning*. Journal of Autoimmunity, 1996. **9**(5): p. 667-675.
23. Walker, L.S.K. and A.K. Abbas, *The enemy within: keeping self-reactive T cells at bay in the periphery*. Nat Rev Immunol, 2002. **2**(1): p. 11-19.
24. Bouneaud, C., P. Kourilsky, and P. Bousso, *Impact of negative selection on the T cell repertoire reactive to a self-peptide: a large fraction of T cell clones escapes clonal deletion*. Immunity, 2000. **13**(6): p. 829-40.
25. Lenschow, D.J., T.L. Walunas, and J.A. Bluestone, *CD28/B7 system of T cell costimulation*. Annual review of immunology, 1996. **14**(1): p. 233-258.
26. Zhang, H.-g., et al., *Induction of specific T cell tolerance by Fas ligand-expressing antigen-presenting cells*. The Journal of Immunology, 1999. **162**(3): p. 1423-1430.
27. Wajant, H., *The Fas Signaling Pathway: More Than a Paradigm*. Science, 2002. **296**(5573): p. 1635-1636.
28. Nishimura, H., et al., *Development of Lupus-like Autoimmune Diseases by Disruption of the *PD-1* Gene Encoding an ITIM Motif-Carrying Immunoreceptor*. Immunity, 1999. **11**(2): p. 141-151.
29. Freeman, G.J., et al., *Engagement of the Pd-1 Immunoinhibitory Receptor by a Novel B7 Family Member Leads to Negative Regulation of Lymphocyte Activation*. The Journal of Experimental Medicine, 2000. **192**(7): p. 1027-1034.
30. Piccirillo, C.A. and E.M. Shevach. *Naturally-occurring CD4<sup>+</sup> CD25<sup>+</sup> immunoregulatory T cells: central players in the arena of peripheral tolerance*. Elsevier.
31. Beissert, S., A. Schwarz, and T. Schwarz, *Regulatory T cells*. Journal of investigative dermatology, 2006. **126**(1): p. 15-24.
32. Gardner, J.M., et al., *Deletional Tolerance Mediated by Extrathymic Aire-Expressing Cells*. Science, 2008. **321**(5890): p. 843-847.
33. Schönrich, G., et al., *Down-regulation of T cell receptors on self-reactive T cells as a novel mechanism for extrathymic tolerance induction*. Cell, 1991. **65**(2): p. 293-304.
34. Murphy, M., et al., *Expression of the lymphotoxin beta receptor on follicular stromal cells in human lymphoid tissues*. Cell Death Differ, 1998. **5**(6): p. 497-505.
35. Chang, Y.H., et al., *Lymphotoxin beta receptor induces interleukin 8 gene expression via NF-kappaB and AP-1 activation*. Exp Cell Res, 2002. **278**(2): p. 166-74.
36. Chapoval, A.I., et al., *B7-H3: a costimulatory molecule for T cell activation and IFN-γ production*. Nature immunology, 2001. **2**(3): p. 269-274.
37. Lu, Y., et al., *IFN-γ and indoleamine 2, 3-dioxygenase signaling between donor dendritic cells and T cells regulates graft versus host and graft versus leukemia activity*. Blood, 2012. **119**(4): p. 1075-1085.
38. Gao, J., et al., *An interferon-γ-activated site (GAS) is necessary for full expression of the mouse iNOS gene in response to interferon-γ and lipopolysaccharide*. Journal of biological chemistry, 1997. **272**(2): p. 1226-1230.
39. Meisel, R., et al., *Human bone marrow stromal cells inhibit allogeneic T-cell responses by indoleamine 2, 3-dioxygenase-mediated tryptophan degradation*. Blood, 2004. **103**(12): p. 4619-4621.
40. Fallarino, F., et al., *T cell apoptosis by kynurenines*, in *Developments in tryptophan and serotonin metabolism*. 2003, Springer. p. 183-190.

41. Terness, P., et al., *Inhibition of Allogeneic T Cell Proliferation by Indoleamine 2, 3-Dioxygenase-expressing Dendritic Cells Mediation of Suppression by Tryptophan Metabolites*. The Journal of experimental medicine, 2002. **196**(4): p. 447-457.
42. Lu, P., et al., *Critical Role of TNF- $\alpha$ -Induced Macrophage VEGF and iNOS Production in the Experimental Corneal Neovascularization*. Investigative Ophthalmology & Visual Science, 2012. **53**(7): p. 3516-3526.
43. de Vera, M.E., et al., *Transcriptional regulation of human inducible nitric oxide synthase (NOS2) gene by cytokines: initial analysis of the human NOS2 promoter*. Proceedings of the National Academy of Sciences, 1996. **93**(3): p. 1054-1059.
44. Lipton, S.A., et al., *A redox-based mechanism for the neuroprotective and neurodestructive effects of nitric oxide and related nitroso-compounds*. 1993.
45. Niedbala, W., B. Cai, and F. Liew, *Role of nitric oxide in the regulation of T cell functions*. Annals of the rheumatic diseases, 2006. **65**(suppl 3): p. iii37-iii40.
46. von Andrian, U.H. and T.R. Mempel, *Homing and cellular traffic in lymph nodes*. Nat Rev Immunol, 2003. **3**(11): p. 867-878.
47. Turley, S.J., A.L. Fletcher, and K.G. Elpek, *The stromal and haematopoietic antigen-presenting cells that reside in secondary lymphoid organs*. Nat Rev Immunol, 2010. **10**(12): p. 813-825.
48. Link, A., et al., *Fibroblastic reticular cells in lymph nodes regulate the homeostasis of naive T cells*. Nature immunology, 2007. **8**(11): p. 1255-1265.
49. Chai, Q., et al., *Maturation of Lymph Node Fibroblastic Reticular Cells from Myofibroblastic Precursors Is Critical for Antiviral Immunity*. Immunity, 2013. **38**(5): p. 1013-1024.
50. Petrova, T.V., et al., *Lymphatic endothelial reprogramming of vascular endothelial cells by the Prox-1 homeobox transcription factor*. The EMBO journal, 2002. **21**(17): p. 4593-4599.
51. Podgrabinska, S., et al., *Molecular characterization of lymphatic endothelial cells*. Proceedings of the National Academy of Sciences, 2002. **99**(25): p. 16069-16074.
52. Gunn, M.D., et al., *A chemokine expressed in lymphoid high endothelial venules promotes the adhesion and chemotaxis of naive T lymphocytes*. Proceedings of the National Academy of Sciences, 1998. **95**(1): p. 258-263.
53. Banchereau, J. and R.M. Steinman, *Dendritic cells and the control of immunity*. Nature, 1998. **392**(6673): p. 245-252.
54. Fletcher, A.L., et al., *Reproducible isolation of lymph node stromal cells reveals site-dependent differences in fibroblastic reticular cells*. Frontiers in immunology, 2011. **2**.
55. Ye, J., et al., *Primer-BLAST: A tool to design target-specific primers for polymerase chain reaction*. BMC Bioinformatics, 2012. **13**(1): p. 134.
56. Ehmann, U.K., et al., *An in vitro model of epithelial cell growth stimulation in the rodent mammary gland*. Cell Prolif, 2003. **36**(4): p. 177-90.
57. Darby, I., O. Skalli, and G. Gabbiani, *Alpha-smooth muscle actin is transiently expressed by myofibroblasts during experimental wound healing*. Laboratory investigation; a journal of technical methods and pathology, 1990. **63**(1): p. 21-29.
58. Banerji, S., et al., *LYVE-1, a new homologue of the CD44 glycoprotein, is a lymph-specific receptor for hyaluronan*. The Journal of cell biology, 1999. **144**(4): p. 789-801.
59. Kondziolka, D. and J.M. Bilbao, *An immunohistochemical study of neuroepithelial (colloid) cysts*. Journal of neurosurgery, 1989. **71**(1): p. 91-97.
60. Caux, C., et al., *Activation of human dendritic cells through CD40 cross-linking*. The Journal of experimental medicine, 1994. **180**(4): p. 1263-1272.

61. Yang, L., et al., *ICAM-1 regulates neutrophil adhesion and transcellular migration of TNF- $\alpha$ -activated vascular endothelium under flow*. *Blood*, 2005. **106**(2): p. 584-592.
62. Lanier, L.L., et al., *CD80 (B7) and CD86 (B70) provide similar costimulatory signals for T cell proliferation, cytokine production, and generation of CTL*. *The Journal of Immunology*, 1995. **154**(1): p. 97-105.
63. Springer, T.A., *Traffic signals for lymphocyte recirculation and leukocyte emigration: the multistep paradigm*. *Cell*, 1994. **76**(2): p. 301-314.
64. Chemnitz, J.M., et al., *SHP-1 and SHP-2 associate with immunoreceptor tyrosine-based switch motif of programmed death 1 upon primary human T cell stimulation, but only receptor ligation prevents T cell activation*. *J Immunol*, 2004. **173**(2): p. 945-54.
65. Keir, M.E., et al., *Tissue expression of PD-L1 mediates peripheral T cell tolerance*. *The Journal of experimental medicine*, 2006. **203**(4): p. 883-895.
66. Zhang, Y., et al., *Regulation of T cell activation and tolerance by PDL2*. *Proceedings of the National Academy of Sciences*, 2006. **103**(31): p. 11695-11700.
67. Wang, S., et al., *Costimulation of T cells by B7-H2, a B7-like molecule that binds ICOS*. *Blood*, 2000. **96**(8): p. 2808-2813.
68. Lund, F.E., et al., *CD38: a new paradigm in lymphocyte activation and signal transduction*. *Immunological reviews*, 1998. **161**(1): p. 79-93.
69. Stamenkovic, I., et al., *The hematopoietic and epithelial forms of CD44 are distinct polypeptides with different adhesion potentials for hyaluronate-bearing cells*. *The EMBO journal*, 1991. **10**(2): p. 343.
70. Gojo, S., et al., *In vivo cardiovascularogenesis by direct injection of isolated adult mesenchymal stem cells*. *Experimental cell research*, 2003. **288**(1): p. 51-59.
71. Itoh, M., et al., *Deletion of bone marrow stromal cell antigen-1 (CD157) gene impaired systemic thymus independent-2 antigen-induced IgG3 and mucosal TD antigen-elicited IgA responses*. *The Journal of Immunology*, 1998. **161**(8): p. 3974-3983.
72. Sugiyama, T., et al., *Maintenance of the hematopoietic stem cell pool by CXCL12-CXCR4 chemokine signaling in bone marrow stromal cell niches*. *Immunity*, 2006. **25**(6): p. 977-988.
73. Lamoury, F., J. Croitoru-Lamoury, and B. Brew, *Undifferentiated mouse mesenchymal stem cells spontaneously express neural and stem cell markers Oct-4 and Rex-1*. *Cytotherapy*, 2006. **8**(3): p. 228-242.
74. Okada, S., et al., *In vivo and in vitro stem cell function of c-kit-and Sca-1-positive murine hematopoietic cells*. *Blood*, 1992. **80**(12): p. 3044-3050.
75. Oka, M., et al., *CD9 is associated with leukemia inhibitory factor-mediated maintenance of embryonic stem cells*. *Molecular biology of the cell*, 2002. **13**(4): p. 1274-1281.
76. Shackleton, M., et al., *Generation of a functional mammary gland from a single stem cell*. *Nature*, 2006. **439**(7072): p. 84-88.
77. Heinzl, F.P., et al., *Reciprocal expression of interferon gamma or interleukin 4 during the resolution or progression of murine leishmaniasis. Evidence for expansion of distinct helper T cell subsets*. *The Journal of experimental medicine*, 1989. **169**(1): p. 59-72.
78. Mannering, S.I., et al., *A sensitive method for detecting proliferation of rare autoantigen-specific human T cells*. *Journal of immunological methods*, 2003. **283**(1): p. 173-183.
79. Oehen, S. and K. Brduscha-Riem, *Differentiation of naive CTL to effector and memory CTL: correlation of effector function with phenotype and cell division*. *The Journal of Immunology*, 1998. **161**(10): p. 5338-5346.
80. Moretta, A., R.S. Accolla, and J.-C. Cerottini, *IL-2-mediated T cell proliferation in humans is blocked by a monoclonal antibody directed against monomorphic determinants of HLA-DR antigens*. *The Journal of experimental medicine*, 1982. **155**(2): p. 599-604.

81. Locke, M., J. Windsor, and P.R. Dunbar, *Human adipose-derived stem cells: isolation, characterization and applications in surgery*. ANZ J Surg, 2009. **79**(4): p. 235-44.
82. Zuk, P.A., et al., *Human adipose tissue is a source of multipotent stem cells*. Molecular biology of the cell, 2002. **13**(12): p. 4279-4295.
83. Kong, Y.-Y., et al., *Activated T cells regulate bone loss and joint destruction in adjuvant arthritis through osteoprotegerin ligand*. Nature, 1999. **402**: p. 43-47.
84. Aruffo, A., et al., *CD44 is the principal cell surface receptor for hyaluronate*. Cell, 1990. **61**(7): p. 1303-1313.
85. Jones, R., M. Jacobson, and W. Steudel, *alpha-smooth-muscle actin and microvascular precursor smooth-muscle cells in pulmonary hypertension*. Am J Respir Cell Mol Biol, 1999. **20**(4): p. 582-94.
86. Dominici, M., et al., *Minimal criteria for defining multipotent mesenchymal stromal cells. The International Society for Cellular Therapy position statement*. Cytotherapy, 2006. **8**(4): p. 315-317.
87. Gavard, J. and J.S. Gutkind, *VEGF controls endothelial-cell permeability by promoting the beta-arrestin-dependent endocytosis of VE-cadherin*. Nature cell biology, 2006. **8**(11): p. 1223-1234.
88. Bardin, N., et al., *Identification of CD146 as a component of the endothelial junction involved in the control of cell-cell cohesion*. Blood, 2001. **98**(13): p. 3677-3684.
89. Jackson, D.G., et al., *LYVE-1, the lymphatic system and tumor lymphangiogenesis*. Trends in immunology, 2001. **22**(6): p. 317-321.
90. Cursiefen, C., et al., *Lymphatic vessels in vascularized human corneas: immunohistochemical investigation using LYVE-1 and podoplanin*. Investigative ophthalmology & visual science, 2002. **43**(7): p. 2127-2135.
91. Akashi, K., M. Kondo, and I.L. Weissman, *Role of interleukin-7 in T-cell development from hematopoietic stem cells*. Immunol Rev, 1998. **165**: p. 13-28.
92. Koch, A.E., et al., *Interleukin-8 as a macrophage-derived mediator of angiogenesis*. Science, 1992. **258**(5089): p. 1798-1801.
93. Schmitt, T.M., et al., *Maintenance of T Cell Specification and Differentiation Requires Recurrent Notch Receptor–Ligand Interactions*. The Journal of Experimental Medicine, 2004. **200**(4): p. 469-479.
94. Shearer, W.T., et al., *Biology of common beta receptor–signaling cytokines: IL-3, IL-5, and GM-CSF*. Journal of Allergy and Clinical Immunology, 2003. **112**(4): p. 653-665.

CURRICULUM VITAE  
Nicholas J. Stoffel

**Education:**

2008	B.S. Biology Minor in Chemistry Indiana-Purdue University Fort Wayne	Fort Wayne, IN
2013	M.S. Microbiology and Immunology Indiana University	Indianapolis, IN

**Activities and Honors:**

2004-2008	Dean's List
2006-2008	Beta Beta Beta Biological Honors Society
2007-2008	Biological Sciences Club Vice President
2011-2012	University Fellowship Travel Award
2012-2013	Graduate Student Mentor
2012-2013	IBMG 2 <sup>nd</sup> Year Fellowship Award
2013	Volunteer: St. Vincent Emergency Department
2013	Volunteer: Second Helpings Food Bank
2013	Volunteer: Wheeler Mission Men's Residential Center
2013	Volunteer: Big Brothers Big Sisters

**Work Experience:**

2008	Walgreens Pharmacy Technician <ul style="list-style-type: none"><li>• Performed data entry</li><li>• Processed customer insurance</li><li>• Filled prescriptions</li></ul>
2010-2011	American Institute of Toxicology Chemist I <ul style="list-style-type: none"><li>• Operated HPLC and MS instruments</li><li>• Integrated and analyzed forensic and pain patients' samples for drugs of interest</li></ul>